Effect of inorganics on the thermal decomposition behaviour of wheat straw

José Miguel da Vinha Pereira Penedos

Thesis to obtain the Master of Science Degree in

Mechanical Engineering

Supervisors: Prof. Miguel Abreu de Almeida Mendes

Dr. Raquel Inês Segurado Correia Lopes da Silva

Examination Committee

Chairperson: Prof. José Manuel da Silva Chaves Ribeiro Pereira

Supervisor: Dr. Raquel Inês Segurado Correia Lopes da Silva

Member of the Committee: Prof. Paulo Sérgio Duque de Brito

October 2021

Acknowledgments

Throughout the writing of this dissertation, I have received a great deal of support and assistance

I would first like to thank my supervisors, Prof. Miguel Mendes and Dr. Raquel Segurado for their knowledge and guidance. I would also like to thank Manuel Pratas and Isabel Ferreiro for all their availability and willingness to help, as well as my colleagues from the Combustion Laboratory, Rodrigo, Ricardo and Tomás for their great companionship.

Finally, I would like to sincerely thank my parents, family, and friends for their unconditional support and belief in me. Without them none of this would be possible.

Resumo

Recentemente, na área da biomassa, tem havido um interesse crescente nos processos termoquímicos para a produção de biocombustíveis. A biomassa geralmente contém minerais nas suas cinzas, o que pode afetar significativamente o seu comportamento em processos de conversão térmica. Esta tese investiga a influência das cinzas na pirólise e gaseificação da palha de trigo. Palha de trigo crua, desmineralizada e dopada com 11.7%, 4.7% e 22.4% de teor de cinzas, respetivamente, foram usadas neste estudo. Os processos de desmineralização através de água foram testados e avaliados quanto à eficácia de remoção de cinzas por meio de análises aproximadas de amostras de palha de trigo. A estrutura química da palha de trigo desmineralizada permaneceu inalterada pelo processo de desmineralização. A palha dopada foi obtida por impregnação a seco da palha crua com cinzas. As cinzas foram determinadas a temperaturas entre os 550ºC e os 1050ºC. O conteúdo de cinza da palha determinada a 1050ºC foi 15,6% menor para a palha crua e cerca de 18% menor para a palha desmineralizada. Curvas termogravimétricas foram obtidas para as amostras a uma taxa de aquecimento de 5ºC / min em uma atmosfera inerte de azoto. As curvas termogravimétricas (TG) mostraram que a impregnação a seco das cinzas não afetou o comportamento pirolítico da palha do trigo. Palha de trigo desmineralizada apresentou uma formação sólidos muito menor em relação à palha de trigo dopada e palha de trigo crua e pareceu sofrer degradação térmica a temperaturas superiores. As curvas termogravimétricas diferenciais (DTG) demonstraram que o pico de degradação térmica da palha de trigo desmineralizada foi parcialmente dividido em dois estágios de decomposição, que foram atribuídos à decomposição da hemicelulose e da celulose. Parâmetros cinéticos de primeira ordem foram obtidos com base em ajustes experimentais. A energia de ativação da palha crua e dopada foi muito semelhante, sendo 79.7 kJ / mol para a palha crua e 79 kJ / mol para a palha dopada, respetivamente, enquanto a palha desmineralizada sofreu um aumento para 99.4 kJ / mol. A gaseificação de palha de trigo crua e desmineralizada foi investigada num forno de queda tubular sob atmosfera de ar entre as temperaturas de operação de 900 e 1200 ° C e excesso de ar de cerca de 0,4. O aumento da temperatura de operação favoreceu a presença de espécies de CO e H2 em detrimento de CH4 e CO2. As altas temperaturas também aumentam claramente a conversão de carbono, já que o rendimento de sólidos foi notoriamente menor para temperaturas mais altas. Contudo, o impacto das cinzas não foi percetível.

Palavras-chave:

Biomassa, Palha de trigo, Pirólise, Cinzas, Termogravimetria, Gasificação, Análise Aproximada

Abstract

Recently in the biomass energy field, there has been a growing interest on thermochemical processes for the production of biofuel. Biomass contains mineral matter in its ashes, which may significantly affect its thermal conversion behavior. This thesis reports the influence of ashes on wheat straw (WS) pyrolysis and gasification. Raw, demineralized and doped wheat straw with 11.7 wt.% db, 4.7 wt.% db and 22.4 wt.% db of ash content, respectively, were used in this study. Water leaching processes were tested and evaluated for ash removal efficacy through proximate analysis of samples. Demineralized WS chemical structure appeared to remain unchanged by the demineralization process. Doped WS was obtained by dry impregnation of raw WS with ashes. WS ashes were determined at temperatures between 550ºC and 1050ºC. WS ash content determined at 1050ºC was 15.6% lower for raw WS and about 18% lower for demineralized WS. Thermogravimetric curves were obtained at a heating rate of 5ºC/min in an inert atmosphere of Nitrogen. The thermogravimetric (TG) curves showed that dry impregnation of ashes did not have any effect on pyrolysis behavior of wheat straw. Demineralized WS presented a much lower solid yield than that of raw and doped WS and appeared to thermally degrade at higher temperatures. The differential thermogravimetric (DTG) curves demonstrated that the thermal degradation peak of demineralized WS was partially split into two decomposition stages, which were attributed to the decomposition of hemicellulose and cellulose. First order kinetic parameters were obtained based on experimental fittings. Activation energy of raw and doped straw was very similar at 79.7 kJ/mol and 79 kJ/mol, respectively, whereas demineralized straw suffered an increase to 99.4 kJ/mol. Demineralization process appears to have removed some inorganic elements which benefited the thermal decomposition of wheat straw. Gasification of raw and demineralized WS in a drop tube furnace was investigated under atmosphere of air between operating temperatures of 900 and 1200 °C and excess air of about 0.4. Increase of operating temperature favored presence of CO and H2 species in detriment of CH4 and CO2. High temperatures also clearly enhance carbon conversion, as solid yield was notoriously lower for higher temperatures. Impact of ashes, however, was not perceptible.

Keywords:

Biomass, Wheat straw, Pyrolysis, Ashes, Thermogravimetry, Gasification, Proximate analysis

Table of Contents

List of Figures

List of Tables

Nomenclature

Acronyms

GDP	Gross Domestic Product
GHG	Greenhouse Gas
IPCC	Intergovernmental Panel on Climate Change
FTIR	Fourier-transform Infrared Spectroscopy
MIR	Mid Infrared Region
IR	Infrared
TGA	Thermogravimetric Analysis
TG	Thermogravimetric
DTG	Differential Thermogravimetric
WWB	Wood and Woody Biomass
HAB	Herbaceous and Agricultural Biomass
HAS	Herbaceous and Agricultural Straws
HAR	Herbaceous and Agricultural Residues
LHV	Lower Heating Value
PAH	Polycyclic Aromatic Hydrocarbons
WS	Wheat Straw
DTF	Drop Tube Furnace
HTA	High Temperature Ashes
LTA	Low Temperature Ashes
STA	Simultaneous Thermal Analyzer
db	dry basis
daf	dry ash free
M	Moisture
FC	Fixed Carbon
VM	Volatile matter

Symbols

α	Conversion degree	
n	Reaction order	
λ	Excess air coefficient	
k	Reaction rate	(s^{-1})
k_0	Pre-exponential factor	(s^{-1})
E_a	Activation energy	($kJ.mol^{-1}$)
R	Ideal gas constant	($kJ.K^{-1}.mol^{-1}$)
T	Temperature	(K)
β	Heating Rate	(K/s)
ρ_b	Biomass bulk density	(kg/m^3)
M_b	Biomass mass	(kg)
V_c	Container density	(m^3)

1. Introduction

1.1 Motivation

1.1.1 Energy demand

Energy and population are intimately interdependent. Abundant and high-quality energy allows for population growth in size and development, which in turn, creates demand for more energy and higher quality sources. Nowadays, whilst population remains somewhat stagnant in developed nations, growing populations in developing countries are leading to projected increases in world energy consumption. World population is expected to increase from around 7.6 billion in 2018 to approximately 9.8 billion in 2050 [1]. Similarly to population size, increasing urbanization also tends to raise demand for modern forms of energy, as such forms of energy are more accessible in urban areas, where levels of income and economic activity are usually higher. Urbanization rate is expected to grow from 55% in 2018 to 68% in 2050 [1]. Also, as countries and their populations become wealthier, their lifestyles improve, and they subsequently use more energy. According to International Energy Outlook 2019, world GDP is projected to grow anywhere from 77% to 118% between 2018 and 2050 [2]. In all the scenarios considered, world GDP severely increases driven by increasing prosperity in fast-growing developing economies. World primary energy consumption is, therefore, expected to grow by nearly 50% between 2018 and 2050 (Figure 1), with renewables having a projected growth of almost 180% [2].

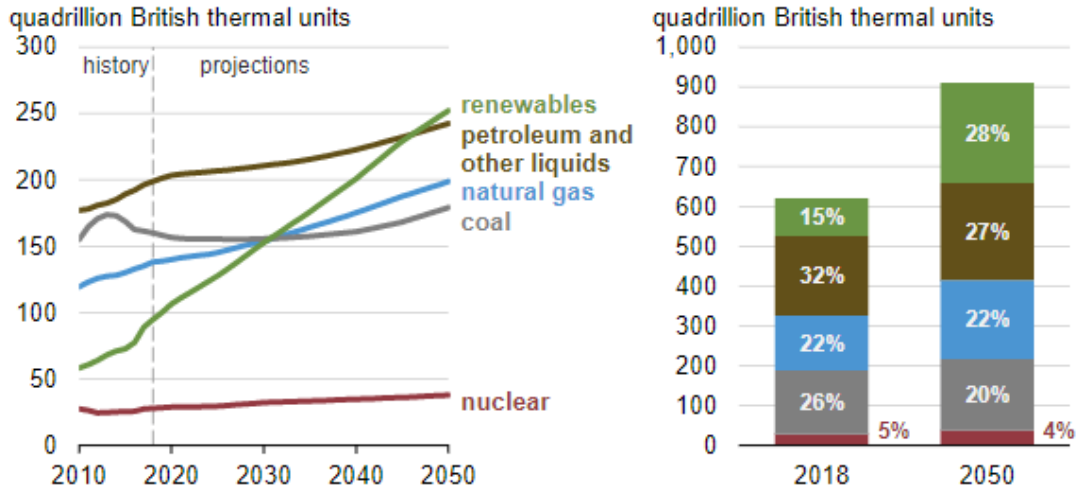

Figure 1. Global primary energy consumption by source between 2010 and 2050 [2].

The combined effect of the ever-increasing population size, density and economic activity will drive demand of affordable and easily accessible energy in the coming decades. Keeping up with this demand in a sustainable and environmentally friendly way will be one of the most pressing challenges of this century.

1.1.2 Renewable energy

For many countries, increasing the share of the population with access energy resources is a main priority, and to do so, low-cost, and easily available energy is essential. In this regard, fossil fuels have dominated for a long time and are presently still the major energy source, representing about 84% of primary energy consumption worldwide [3]. Fossil fuels are however limited in supply and are closely connected with several environmental problems that have become increasingly noticeable in recent years. Combustion of fossil fuels releases - among other gases - carbon dioxide into the atmosphere, a gas that contributes substantially to the greenhouse effect, aggravating climate change and global warming. The vast majority of anthropogenic GHG emissions come from combustion of fossil fuels. Between 1970 and 2018 GHG emissions have increased around 108% (25 $GtCO_2eq$ to 52 $GtCO_2eq$), being that in 2018 the burning of fossil fuels alone comprised about 64% of total GHG emissions [4]. Human activities are estimated to have caused approximately 1.0°C of global warming above pre-industrial levels. With current emission rates, average global temperatures are expected to rise 1.5ºC above pre-industrial levels between 2030 and 2052 (Figure 2), an increase the United Nations Intergovernmental Panel on Climate Change (IPCC) believe should be adopted as the upper limit for global warming to avoid dangerous temperature levels and major climatical consequences [5].

Given that both energy consumption and fossil fuel depletion are poised to continuing rising in the coming decades and the fact that GHG emissions must be reduced to meet the goals of sustainable development there has been a growing interest in furthering the development of renewable energy.

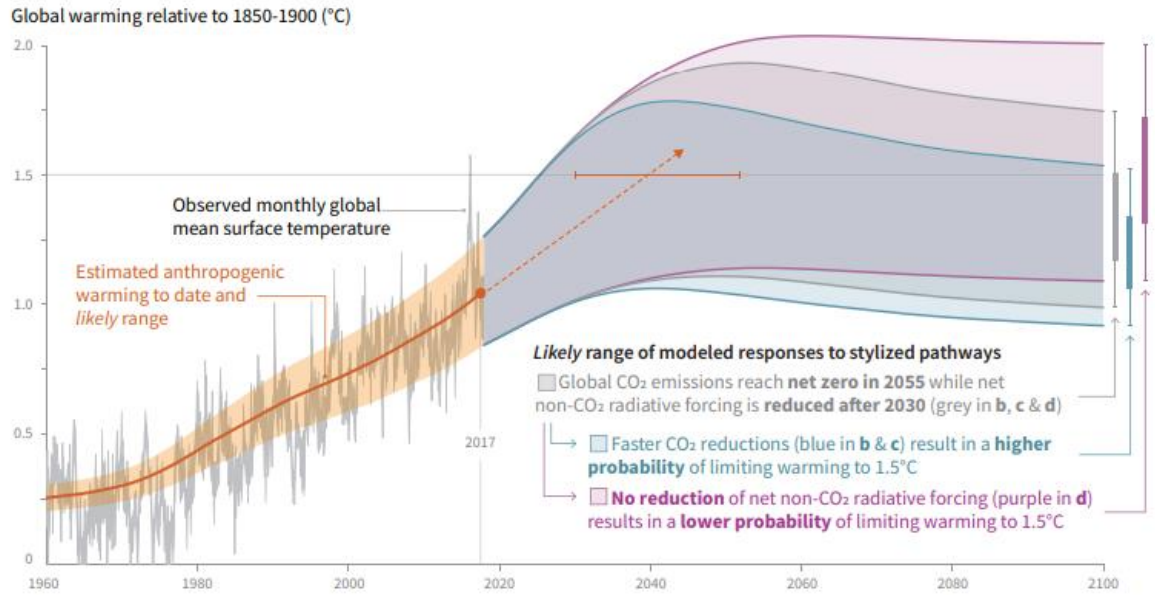

Figure 2.Global Warming Levels between 1960 and 2100 [5].

Currently, among all renewables, hydropower is the largest energy source worldwide, but its share of total renewable energy generation has been steadily declining in recent years due to

technological innovations and improvements in other renewable energy sources such as solar and wind, whose share have - inversely - been increasing. Together, wind, solar and hydropower make up about 90.73% of global renewable energy generation [6]. While these energy sources might have high efficiencies from an energy or cost perspective, they cannot provide reliable power continuously as they are extremely dependent on weather conditions which are particularly volatile - wind is not always blowing, sun is not always shining and resources of water in reservoirs are not always sufficient to meet demand. Biomass energy, in contrast, can provide power or heat continuously if there is a steady supply of biomass which, due to its abundance is generally not a problem. It is also very versatile; while other energy sources can provide electrical or thermal power, biomass can deliver both through direct combustion as well as chemical feedstock and gaseous or liquid fuels through specific thermal conversion processes which will be discussed later. This is one of the most compelling advantages of biomass energy.

1.1.3 Biomass thermal conversion processes

"Biomass refers to non-fossilized and biodegradable organic material originating from plants, animals, and micro-organisms." [7] Unlike fossil fuels, it can easily be replenished (through the biomass cycle) and does not take millions of years to develop. Adding to this, biomass energy is considered as carbon neutral – energy with zero net GHG emissions - since it is a natural part of the carbon cycle, meaning that the carbon released into the atmosphere was absorbed by plants during their lifecycles and thus the net addition of carbon dioxide is zero [7]. Although this might be true in a general sense, some people argue that the process has the potential to be carbon neutral over very long time scales but not in the short term as the burning of biomass releases large amounts of carbon into the atmosphere in a very short amount of time when compared to time required for biomass to draw the same amount of carbon from the atmosphere [8]. Nevertheless, biomass energy is regarded as a renewable, sustainable, and low carbon energy that can deliver nearly everything that fossil fuels provide, whether fuel or chemical feedstock.

Raw biomass presents, however, a rather bulky and inconvenient shape when it comes to handling, storage, and transportation. Unlike solids, liquid and gases are easier to handle because they continuously deform under shear stress - taking the shape of any vessel they are kept in. This provides the main motivation for biomass conversion into liquid and/or gaseous products. Besides its troublesome shape, biomass has high oxygen-carbon and hydrogen-carbon ratios due to the large amounts of oxygen and moisture in its composition [9]. This high percentage of noncombustible material coupled with raw biomass' considerable volume translate inevitably into a fuel with a low heating value and low energy density. For industries where electrification is not an option or presents a major challenge, use of biomass-derived fuels may represent a reasonable alternative to fossil-based fuels. Sustainable production of biofuels is, therefore, essential for a transition towards a low carbon energy future.

Conversion of biomass can be achieved by biochemical or thermochemical processes, depending on the nature of the decomposing agents. In biochemical conversion the biomass is

decomposed by bacteria or enzymes through processes like fermentation, aerobic digestion, and anaerobic digestion, whereas in thermochemical conversion the biomass is decomposed by heat through processes such as combustion, liquefaction, pyrolysis, and gasification.

Recently in the biomass field, there has been a growing interest on thermochemical processes to produce biofuel. Biomass contains mineral matter which may significantly affect its thermal conversion behaviour. It is therefore important to understand the degree to which this mineral matter may improve or degrade the thermal conversion of biomass. This study focuses on thermal conversion of wheat-straw, which represents a major by-product of agricultural production in Europe [10], and the effect of its inherent mineral matter on such conversion. Specific objectives will be presented in section 1.4.

1.2 Theoretical foundations

1.2.1 Biomass composition

Biomass thermal conversion processes involve pre-steps such as choice of suitable biomass and effective pre-treatments. For this it is necessary to understand the structure of biomass (Figure 3). Lignocellulosic biomass is considered as one of the most economical and abundant renewable resources in the world and whose availability does not significantly impact land use. Its major constituents are cellulose (40%–60%), hemicellulose (20%–40%), and lignin (10%–25%) [11]. The minor components of biomass are extractives and inorganic matter – frequently called ash. Cultivation of plants exclusively for energy production usually resort to this type of biomass since, besides having short growing periods and high yields, it is not part of the human food chain – as the human body cannot digest the lignocellulose in biomass – being, therefore, mainly used as feedstock for conversion processes to produce chemicals and biofuels [7].

Cellulose is the most common organic compound on Earth and the primary structural component of biomass cell walls. It is a long unbranched chain polymer with a high degree of polymerization (~7000-15000) and a large molecular weight. Hemicellulose represents a group of carbohydrates with a branched chain structure and a lower degree of polymerization (~500-3000). Lignin is a complex highly branched polymer and is an integral part of the secondary cell walls of plants. Lignin helps provide rigidity to lignocellulosic materials. While cellulose is a crystalline and strong organic compound with high thermal stability, hemicellulose has a random, amorphous structure with little strength and is rich in branches that are very easy to degrade to volatiles at low temperatures. Together, these components can make up over 90% of lignocellulosic biomass [12].

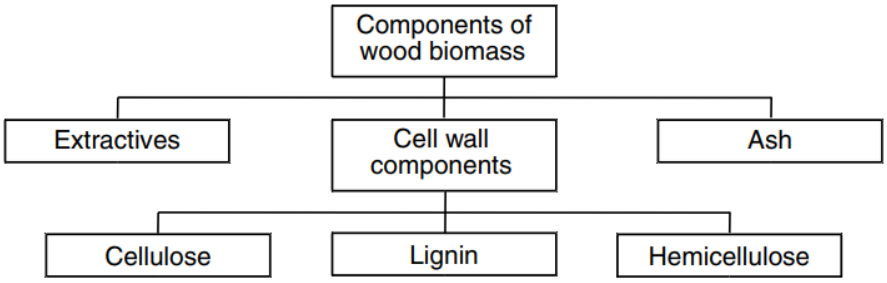

Figure 3.Structural and non-structural components of wood biomass [7].

Extractives are defined as substances that are not an integral part of the biomass structure and can be, therefore, separated by successive treatment with solvents and recovered by evaporation of the solution. Ash refers just to the measured quantity of the incombustible inorganic residue resulting from the complete combustion of biomass. Therefore, ash may not be fully representative of the inorganic matter present in the raw biomass, since, at elevated temperatures, some inorganic elements may volatilize and less stable minerals can decompose [13]. Despite this, ash yield can be easily measured, while the actual determination of bulk inorganic and mineral contents of biomass generally involves difficult processes, that cannot be quickly and routinely achieved. For this reason, ash yield is still an important parameter for evaluating the mineral matter of biomass [14]. Generally, the main elemental constituents of biomass minerals are Si, Ca, K, Na and Mg, with smaller amounts of S, P, Fe, Mn and Al. These constituents occur as oxides, silicates, carbonates, sulfates, chlorides and phosphates. The ash content depends on the amount of organic and inorganic matter and possible impurities in biomass. Although the ash content is reasonably consistent for the same biomass feedstock, its individual constituents vary considerably. This is related to the raw material itself – type of biomass, plant species or plant parts, growth processes and conditions, plant age, fertilization –, the processing methods - harvest time and techniques, transport, and storage conditions – and even the combustion process – fuel preparation, combustion technology and combustion conditions [9], [15].

1.2.2 Biomass characterization

Being a resource that has numerous sources, biomass is generally abundant in its quantity, but extremely varied in its composition and properties. The substantial variability of biomass composition and properties presents a major challenge for conversion processes, which frequently require physically and chemically uniform materials [16]. Hence, major efforts are put into determining biomass composition and properties. For such information specific biomass analysis are conducted.

Ultimate analysis gives the composition of the biomass in terms of its individual elemental constituents, - carbon, hydrogen, oxygen, and nitrogen (see Equation 1). Waste biomass may also have residual quantities of chlorine and sulfur, although these are present in lesser amounts.

$$C + H + O + N + S = 100\% \quad (1)$$

Proximate analysis provides the composition of the biomass in terms of gross components such as moisture, volatile matter, ash, and fixed carbon (see Equation 2). It is a relatively simple and inexpensive process.

$$VM + FC + M + ASH = 100\% \quad (2)$$

Volatile matter (VM) of a fuel is the condensable and noncondensable vapor released when the fuel is heated. The amount of vapor released usually depends on the heating rate and the temperature to which it is heated. Fixed carbon (FC) is the solid carbon in the biomass that remains in the char after devolatilization. Moisture content is one of the most important parameters when using a biomass thermal conversion systems, since it critically affects the energy balance [16]. Ash is the inorganic solid residue left after the fuel is completely burned and is majorly composed of the inorganic matter in biomass.

Fourier-Transform Infrared Spectroscopy (FTIR) is a common technique used to characterize materials by obtaining an infrared (IR) spectrum of absorption of a solid, liquid or gas. When IR radiation is passed through a sample, some radiation is absorbed by the sample and some passes through (is transmitted). The goal is to measure how much light a sample absorbs at each wavelength. Figure 4 [17] shows detector response as transmittance on the y-axis, and IR frequency in terms of wavenumber (cm^{-1}) on the x-axis. Different compounds will peak at different locations on the horizontal axis. Thus, this spectrum acts like a “spectral fingerprint” and enables the identification of the presence of organic and inorganic compounds in the sample. The spectral range of greatest use for chemical analysis is the mid-IR (MIR) region. It covers the frequency range from 4000 to 500 cm^{-1}. This region can be subdivided into the group frequency region, 4000-1 300 cm^{-1} and the fingerprint region, 1300-500 cm^{-1}. Identification of a material using the fingerprint region (1300-500 cm^{-1}) is based on the correlation between the peak pattern of the sample and the peak pattern of a standard material of known chemical composition [18].

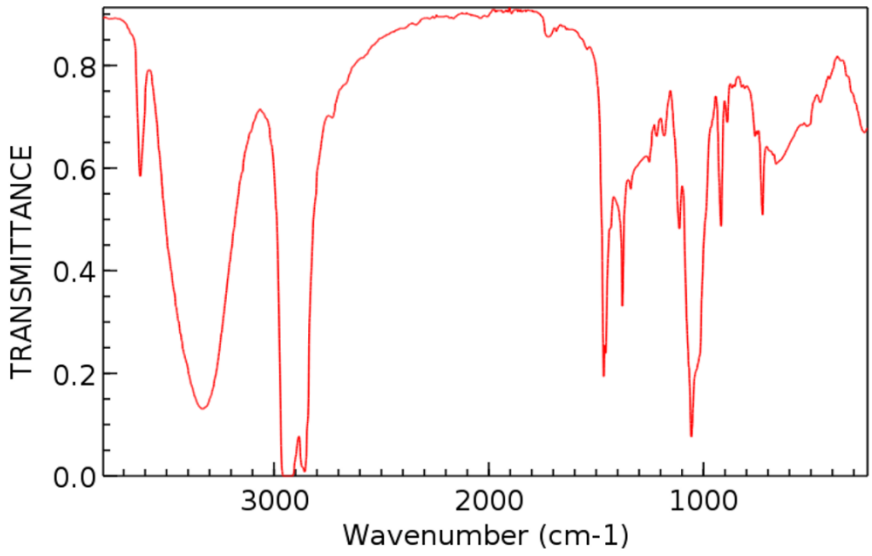

Figure 4.Typical FTIR spectra [17].

1.2.3 Pyrolysis

In thermal fuel conversion of biomass, pyrolysis is an important step which determines separation of the biomass components into several products (char, tar and gas). Figure 5 shows the evolution solid weight fraction with prolonged vapor residence times in a typical pyrolysis process. The pyrolysis process may be represented by a generic reaction such as:

$$C_nH_mO_p(Biomass) \xrightarrow{Heat} \sum_{liquid} C_xH_yO_z + \sum_{gas} C_aH_bO_c + H_2O + C(char) \quad (3)$$

Pyrolysis reactions consist of the thermal breakdown of larger hydrocarbon molecules into smaller gas molecules in the absence of an oxidizing agent. Pyrolysis of biomass is usually carried out at a relatively low temperature, ranging from 250 to 700 ºC [16] and involves heating biomass in an inert atmosphere at a specified rate to a maximum temperature. The devolatilization of biomass usually starts at temperatures as low as 250- 300 °C when the hemicellulose starts to depolymerize. Cellulose undergoes the same processes at a narrower range of temperature around 380 °C whereas lignin, decomposes over a wider range of temperature (300-700 °C) [19].

The reaction scheme of pyrolysis is extremely complex due to the formation of countless intermediate species. In the initial stage (100-300ºC) exothermic dehydrations of biomass occurs, with the release of water and low-molecular-weight gases like CO and CO_2. The initial products of pyrolysis consist of tars, gases, and solid char. Primary pyrolysis takes place in the temperature range of 200 to 600ºC. Large molecules of biomass particles decompose into primary char, condensable gases (vapours and precursors of the liquid yield), and noncondensable gases. The final stage of pyrolysis

involves secondary cracking of volatiles into char and noncondensable gases. If they reside in the biomass long enough, relatively large-molecular-weight condensable gases can crack, yielding additional char (called secondary char) and gases. The tar formed by primary pyrolysis also undergoes secondary thermal decomposition - breaking down further into noncondensable gases and additional liquid and solid products - through gas phase homogeneous reactions and gas-solid phase heterogeneous reactions.[20]

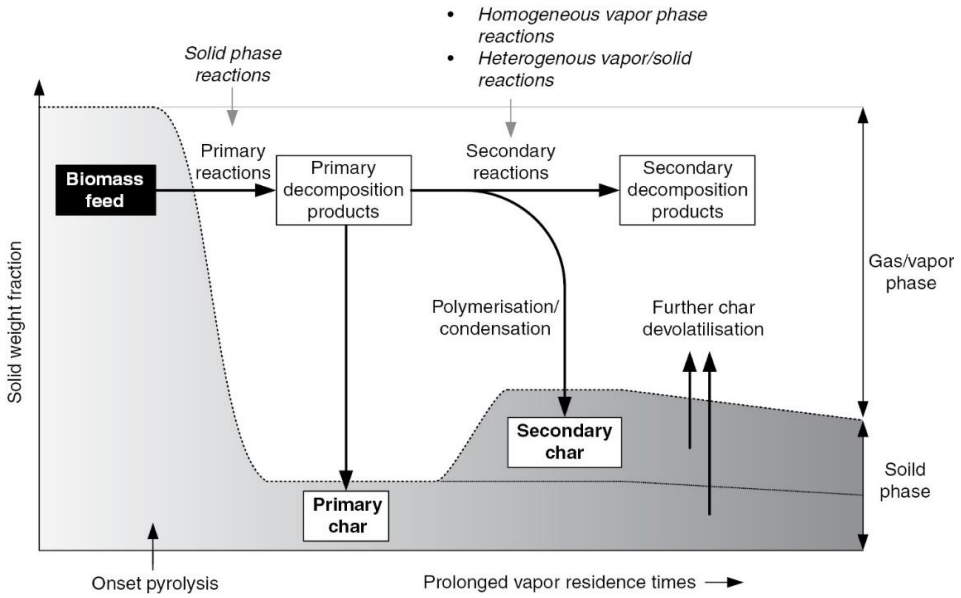

Figure 5. Solid weight fraction evolution [20].

1.2.4 Thermogravimetric analysis

Thermogravimetric Analysis (TGA) is a technique in which the mass of a substance is continuously monitored as a function of temperature or time, as the substance is subjected to controlled temperatures, in a controlled atmosphere, being a very powerful tool in the study of biomass thermal conversion processes, such as pyrolysis. The thermogravimetric data collected is compiled into a plot of mass percentage on the y-axis versus either temperature or time on the x-axis (see Figure 6). From the first derivative of the TG curve - in relation to time or temperature -, the DTG curve can be obtained. In this case, a series of peaks are observed according to the mass loss. The horizontal plateau on the TG curve corresponds to zero in the DTG curve and maximum point on the DTG curve is obtained when the TG curve presents the highest gradient, i.e. where the mass variation occurs more rapidly.

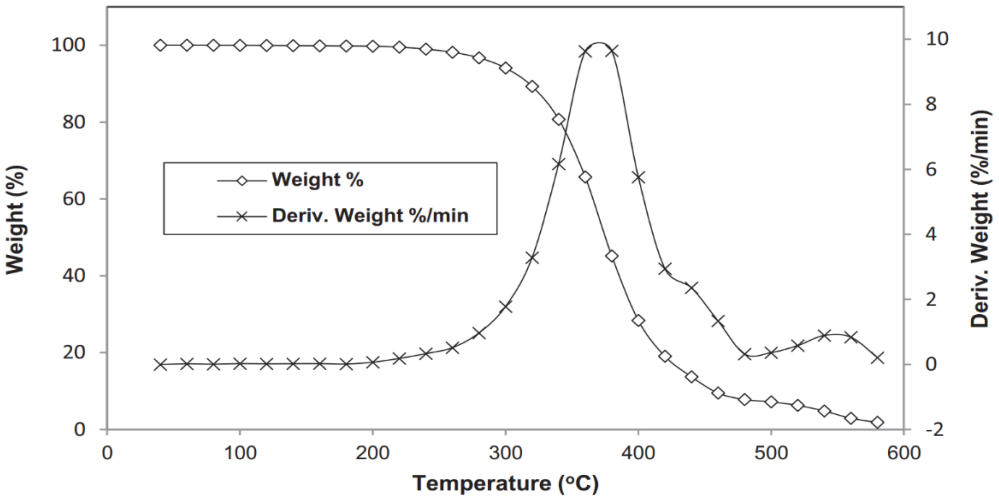

Figure 6.Typical TG and DTG curves. Adapted from [21].

Thermogravimetric kinetics may also be explored for insight into the reaction mechanisms of thermal decomposition involved in biomass pyrolysis. Kinetic models of the pyrolysis of lignocellulosic fuels like biomass may be broadly classified accordingly to the number of species that are taken into consideration. The simplest one is the one-stage global single-reaction model. In this model, pyrolysis is modelled by a one-step reaction using experimentally measured weight-loss rates [7]. This reaction model is based on a single overall reaction:

$$Biomass \xrightarrow{Heat} Volatile + Char \tag{4}$$

Empirical models, based on apparent kinetics, can be used to estimate global kinetic parameters. In the model-fitting methods the reaction models are fitted to the TGA results data and the model with the best correlation is selected as the one from which the apparent activation energy and the pre-exponential factor are estimated. This kind of model is largely used due to its suitability to calculate directly the kinetic parameters from TGA results, having only one heating rate experiment. Within this context, the following kinetic law can be used as a global reaction model for biomass pyrolysis:

$$\frac{d\alpha}{dt} = k\,(1-\alpha)^n \tag{5}$$

where n is the reaction order, α is the conversion degree and k is the reaction rate, given by the following Arrhenius-type law:

$$k = k_0 \exp\left[-{}^{E_a}/_{RT}\right] \quad (6)$$

The Arrhenius equation introduces the relationships between rate and k_0, E_a, R, and T, where k_0 is the pre-exponential factor (s^{-1}), E_a, is the activation energy (kJ/mol), R is the ideal gas constant (kJ/(K.mol)), and T is the temperature (K). The pre-exponential factor, k_0, is also called the frequency factor and describes how often two molecules collide. The activation energy, E_a, is the energy difference between the reactants and the activated complex, also known as transition state (see Figure 7). In a chemical reaction, the transition state is defined as the highest-energy state of the system. If the molecules in the reactants collide with enough kinetic energy and this energy is higher than the transition state energy, then the reaction occurs and products are formed. The activation energy can be, therefore, interpreted as the minimum energy requirement for a chemical reaction to occur. If a catalyst is added to the reaction, the activation energy is lowered because a lower-energy transition state is formed, as shown in Figure 7. The reaction proceeds faster because less energy is required for molecules to react when they collide. Thus, the rate constant increases [22].

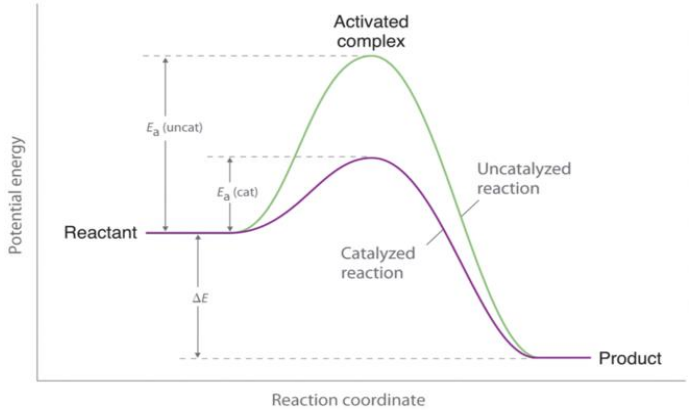

Figure 7.Reaction coordinate diagram for catalyzed and uncatalyzed reactions [22].

Substituting equation 6 into equation 5 results:

$$\frac{d\alpha}{dt} = k_0 \exp\left[-{}^{E_a}/_{RT}\right] (1-\alpha)^n \quad (7)$$

Assuming a non-isothermal reaction with a constant heating rate $\beta = dT / dt$ and introducing it into equation 7 gives:

$$\frac{d\alpha}{(1-\alpha)^n} = \frac{k_0}{\beta}\exp\left[-{E_a}/{RT}\right]\, dT \tag{8}$$

The integration of equation 8 originates:

$$g(\alpha) = \int_0^{\alpha} \frac{d\alpha}{(1-\alpha)^n} = \frac{k_0}{\beta}\int_0^{T} \exp\left[-{E_a}/{RT}\right]\, dT \tag{9}$$

where $g(\alpha)$ is the conversion integral function [23].

Finally, equation 9 can be integrated by using the Coats-Redfern method [23], yielding:

$$\ln\left[\frac{\mathrm{g(\alpha)}}{\mathrm{T^2}}\right] = \ln\left[k_0\frac{R}{\beta E_a}\left(1-\frac{2\mathrm{RT}}{\mathrm{E_a}}\right)\right] - \frac{\mathrm{E_a}}{\mathrm{RT}} \tag{10}$$

As the term $2\mathrm{RT}/\mathrm{E_a}$ is significantly smaller than the unit it can be neglected so that, equation 10 can be written as:

$$\ln\left[\frac{\mathrm{g(\alpha)}}{\mathrm{T^2}}\right] = -\frac{\mathrm{E_a}}{\mathrm{RT}} + \ln\left[\frac{k_0\, R}{\beta E_a}\right] \tag{11}$$

where $g(\alpha)$ is given by:

$$g(\alpha) = \begin{cases} -\ln[1-\alpha], & n = 1 \\ \dfrac{1-(1-\alpha)^{1-n}}{(1-n)}, & n \neq 1 \end{cases} \tag{12}$$

Equation 11 has a linear form. The plot of $\ln\left[\frac{\mathrm{g(\alpha)}}{\mathrm{T^2}}\right]$ vs $\frac{1}{T}$ originates a straight line with a slope of $-\frac{E_a}{R}$ and a y-intercept of $\ln\left[\frac{k_0\,\mathrm{R}}{\beta\,\mathrm{E_a}}\right]$. The apparent activation energy can be determined from the slope of this straight line and the pre-exponential factor from the y-intercept term.

1.2.5 Gasification

Gasification is a thermochemical process that converts carbonaceous materials – like fossil fuels or biomass - into useful gaseous products or chemical feedstock. Unlike combustion, which also produces gaseous products from carbonaceous materials, gasification packs energy into chemical bonds in an oxygen-deficient environment through energy-requiring chemical reactions and its product gas has a useful heating value. It is, in essence, a combustion in which the supply of oxygen is limited and, therefore, the formed gaseous products are not completely oxidized and retain a high chemical potential. Gasification, as a process, strives to control the distinct thermal processes that naturally occur during combustion, manipulating them into producing desired end products. These thermal processes can be seen in Figure 8 and include drying, pyrolysis, combustion and cracking, and reduction [24].

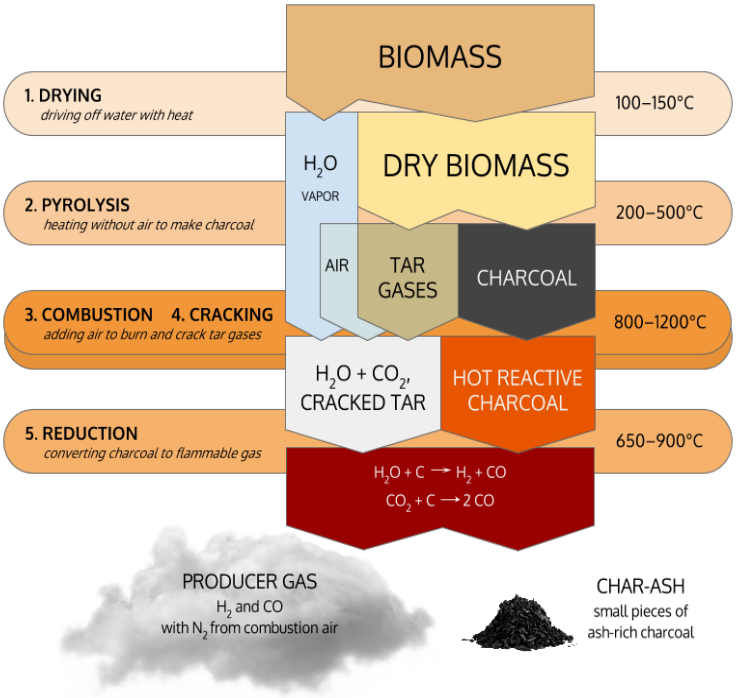

Figure 8.Gasification Overview. (Adapted from [24])

Drying

Drying phase consists in the evaporation of the moisture content of biomass. Typically, temperature in drying zone is about 100–200 °C [7]. It represents an essential step towards the viability of the gasification process, as the energy required to vaporize the moisture in the feedstock is not recovered and biomass can have high moisture content in its composition – up to 63% – which makes this energy loss one that cannot be disregarded [9]. Pre-drying of the biomass is a common pre-step since it maximizes the removal of moisture before entering the gasifier. Most gasification systems use dry biomass with a moisture content of 10 to 20% [7].

Pyrolysis

In this stage the dry biomass is heated in an inert atmosphere. Since no oxygen is present, biomass does not combust, and its chemical compounds are thermally decomposed into liquid/condensed, gaseous and solid products, as described in section 1.2.3. The liquid products – commonly referred to as tars – consist of a mixture of complex condensable hydrocarbons, the gaseous products are mostly volatile gases like hydrogen, carbon monoxide, carbon dioxide and light hydrocarbons such as methane and the solid products include the inert material present in biomass - ashes – and a solid residue enriched in carbon – char. When the time required to heat biomass to the maximum temperature is much longer than the pyrolysis reaction time, the biomass is said to undergo slow pyrolysis. When the opposite happens, it is said to undergo fast pyrolysis. While slow pyrolysis favours production of solid products by heating biomass to a low temperature (450ºC) over an extended period - applying therefore small heating rates -, fast pyrolysis maximizes liquid yield by rapidly heating biomass (1000 to 10,000 °C/s) to a slightly higher peak temperature (650ºC). The product residence times are, therefore, on the order of minutes for slow pyrolysis and seconds or milliseconds for fast pyrolysis [7]. When gaseous products are desired, peak temperature in fast pyrolysis can be further increased (1000ºC).

Combustion

Gasification is a partial oxidation process, meaning less oxygen is used than that which would otherwise be required for complete combustion of the same amount of fuel. Typically, only 20 to 40 percent of the theoretical stoichiometric oxidant is used [7]. In the combustion reactions, the volatile products and char formed in the pyrolysis react with limited oxygen in exothermic oxidation reactions to form carbon dioxide, carbon monoxide, water vapor and other compounds, while concurrently generating the heat needed to gasify the remaining unoxidized fuel – energy required for gasification reactions may also be externally provided. This stage is the only one in the whole gasification process that is entirely exothermic. Also, during this stage, the high temperatures achieved decompose the large tar molecules that pass the combustion zone. Thermal cracking is the process of breaking down large complex molecules such as tar into lighter gases by exposure to heat.

Reduction

In the reduction stage, the carbon in the solid char reacts with the oxygen in the gasifying agent and is converted into energy carrying low-molecular-weight gases – such as CO, H_2 and CH_4. Although gasification and combustion reactions can occur simultaneously in a gasifier, they are in essence two equal and opposite reactions. Combustion comprises oxidation reactions (see Table 1), combining combustible gases with oxygen to release energy and combustion products, whereas gasification comprises reduction reactions, which remove the oxygen from combustion products and store energy in the chemical bonds of the resulting combustible gases. The combustion reaction consumes nearly all of the oxygen feed, so the residual char undergoes gasification reactions in a reducing environment downstream of this zone.

Table 1. Typical Gasification Reactions [7].

Reaction Type	Reaction	Heat of Reaction at 25 ºC (kJ/mol)
Carbon Reactions		
R1 (Boudouard)	$C + CO_2 \leftrightarrow 2CO$	+172
R2 (water-gas or steam)	$C + H_2O \leftrightarrow CO + H_2$	+131
R3 (hydrogasification)	$C + 2H_2 \leftrightarrow CH_4$	-74.8
R4	$C + 0.5O_2 \rightarrow CO$	-111
Oxidation Reactions		
R5	$C + O_2 \rightarrow CO_2$	-394
R6	$CO + 0.5O_2 \rightarrow CO_2$	-284
R7	$CH_4 + 2O_2 \leftrightarrow CO_2 + 2H_2O$	-803
R8	$H_2 + 0.5O_2 \rightarrow H_2O$	-242
Shift Reaction		
R9	$CO + H_2O \leftrightarrow CO_2 + H_2$	-41.2
Methanation Reactions		
R10	$2CO + 2H_2 \rightarrow CH_4 + CO_2$	-247
R11	$CO + 3H_2 \leftrightarrow CH_4 + H_2O$	-206
R12	$CO_2 + 4H_2 \rightarrow CH_4 + 2H_2O$	-165
Steam Reforming Reactions		
R13	$CH_4 + H_2O \leftrightarrow CO + 3H_2$	+206
R14	$CH_4 + 0.5O_2 \rightarrow CO + 2H_2$	-36

1.3 Previous studies

1.3.1 Biomass characterization

There are different groups of biomasses which can be classified as 1) wood and woody biomass (WWB), (2) herbaceous and agricultural biomass (HAB) including straws (HAS) and residues (HAR), (3) aquatic biomass, (4) animal and human biomass wastes, (5) contaminated biomass and industrial biomass wastes. Vassilev et al. [9] performed an extensive study on the composition and application of biomass ash. It was found that the ash yield determined at 550-600 ºC for 86 varieties of biomass ranged from 0.1 to 46 % as received. Mean ash yield for all biomass types was 6.8% and for specific biomass types decreased in the following order: animal biomass (28.8%) > aquatic biomass (21.1%) > contaminated biomass (16.7%) > herbaceous and agricultural biomass (4.4%) > wood and woody biomass (2.7%). Grzegorz Zajac et al. [15] obtained information on the main components of ashes from 35 different biomass species of five different biomass groups. The ash content in the examined biomass samples ranged from 0.37 to 10.44 % as received, with chemical composition of ashes being dominated by macronutrients such as Ca, K, P and S.

In order to study the influence of the mineral content in biomass, leaching procedures using water or acid solutions as leaching agents are generally applied. Das et al. [25] applied treatments for deashing of sugarcane bagasse. The treatments comprised simple water leaching, leaching with 5(M) HCl solution and leaching with hydrogen fluoride (HF) solution ranging between a concentration 0.5 and 3% of HF. Simple water leaching washed out the alkalis like Na and K wherein, 5 M hydrogen chloride (HCl) leaching further removed other alkali metals like Mg, Ca and Al but HF treatment removed almost all the ash elements. While use of acidic solvents was far more efficient in the removal of ash forming elements, their use resulted in the permanent change of chemical structure of biomass. Similar findings were reported by other studies, as Asadieraghi et al. [26] which found that demineralization through diluted acid solutions is effective in removing the inorganic matter from biomass and Jiang et al. [27] verified that the treatment with acid solutions introduces undesirable chemical structure changes in biomass. Mourant et al. [28] applied water and acid washing procedures with deionized water and diluted acid solution of nitric acid (HNO_3) to remove the main alkali and alkaline earth metal species from Malle wood. It was observed that water washing treatments, regardless of their length, were generally quite successful at removing large fractions of the alkaline and earth metal species, with observed reductions of 50 to nearly 100%. However, Mg and Ca could not be completely removed through washing with water. Jenkins et al. [29] deashed rice straw and wheat straw by various water washing techniques – spray washing, flush washing, soak washing and rain washing. K, Na and Cl were easily removed in both tap and distilled water. Total ash was reduced by up to 68% in wheat straw.

1.3.2 Pyrolysis

Commonly, inorganic species are maintained on the char surface instead of being volatized during pyrolysis process. Therefore, they can catalyse the biomass conversion and char formation reactions.

Jensen et al. [30] studied the influence of potassium chloride (KCl) on wheat straw pyrolysis through thermogravimetric Fourier transform infrared (TG-FTIR) analysis. Raw straw, washed straw, and washed straw impregnated with KCl were investigated. While raw straw decomposed in a single peak, results showed that washing straw resulted in the appearance of two peaks in the derivative weight loss curve. It also resulted in a reduction of the char yield from 23 wt. % (daf) to 12 wt. % (daf), and an increase the tar yield from 32 wt. % (daf) to 66 wt. % (daf). The addition of 2 wt. % (daf) of KCl to the washed straw resulted in a char yield which was close to that of the raw straw, and the yields of tar and gases had values between those from the raw and washed straw. Furthermore, the peaks in the derivative weight loss curve moved to lower temperatures but did not collapse to a single peak as in the raw straw. Raveendran et al. [31] studied the effect of mineral matter present in biomass on the pyrolysis characteristics, product distribution and product properties. In total, 13 types of biomasses were studied. Results showed that in general, deashing increased the volatile yield, initial decomposition temperature and rate of pyrolysis.

Pyrolysis of pure wheat straw (WS) and WS doped with several amounts of CaO additives was studied by Han et al. [32] Different heating rates were compared using TG-FTIR analysis. It was shown that increasing amounts of CaO additives resulted in the decrease of the mass loss and maximum mass loss rate in the main devolatilization stage. Unlike pure WS, a second mass loss stage mainly caused by calcium carbonate decomposition appeared in CaO catalysed pyrolysis. Average activation energy of CaO doped samples was lowered and the temperature of maximum mass loss rate was also shifted to a lower value. Pan et al. [33] examined the effect of ion-exchanged cations on wood pyrolysis and reported that K, but not Ca, acted as a catalyst in pyrolytic reactions. Nowakowski et al. [34] studied the influence of K on the pyrolysis behaviour of short rotation willow coppice and synthetic biomass. Results demonstrated that K catalysed pyrolysis increased the char yields markedly and lowered the average apparent first order activation energy for pyrolysis by up to 50 kJ/mol.

1.3.3 Gasification

Billaud et al. [35] conducted beech sawdust gasification experiments in a drop tube furnace (DTF) in the presence of O_2, with temperatures between 800 ºC and 1400 ºC. Results revealed that an increase of the reactor temperature noticeably increased H_2 and CO yields, while CO_2 and H_2O yields decreased. At higher temperatures, reactions R1 and R2 (see Table 1) are favoured (being endothermic in the forward direction) thus explaining the simultaneous increase of CO and H_2 and decrease of CO_2 and H_2O. Several other studies reported similar findings for different values of excess air (λ) biomass type and particle sizes [36], [37]. Zhang et al. [38] investigated tar destruction and soot formation during gasification of biomass for several operating temperatures and gasifying atmospheres. While char and tar yields steadily decreased with increasing temperatures, due to improved char gasification reactions and improved tar cracking reactions – respectively -, soot formation initially increased with temperature until 1100 ºC, but decreased for higher temperatures. Overall, the carbon conversion is augmented with the increase of the temperature.

In general, smaller particle sizes increase the superficial area/volume ratio of the particle, resulting in a more effective mass and heat transfer, which promotes the release of more volatiles during the short period of pyrolysis. Also, higher volatile release results in a more porous and reactive char, which leads to enhanced gasification reactions. In fact, Hernandez et al. [39] verified that decrease of biomass particle size in an entrained flow reactor resulted in higher yields of combustible gases like H_2, CO and CH_4, which directly increased the LHV of the producer gas. As far as particle residence time, the authors verified that longer residence times also increased overall yields of combustible species (CO, H_2, and CH_4) and improved LHV of product gas.

Ash components in biomass have been shown to influence char gasification rates, with alkali metals and alkaline earth metals being the most active constituents [40]. Alkali was hypothesized to reduce the quantity of soot by inhibiting the formation and growth of polycyclic aromatic hydrocarbons (PAH), key intermediates on the formation of soot. Qin et al. [37] investigated the effect operating parameters and biomass types on the syngas composition. Biomass with high K content presented much lower soot

yield. Alkaline earth metals such as K and Ca acted catalytically on the active surface of char improving conversion and the reactivity of the feedstock. Perander et al. [41] studied the catalytic effect of Ca and K on CO_2 gasification of spruce wood. Results revealed that the reactivity increased linearly with the content of K or Ca in the feedstock. Alkali was found to catalyse heterogeneous char gasification reactions and to lead to much lower yields of C2 hydrocarbons, heavy tars, and soot, favouring the presence of lighter species over large aromatic clusters.

1.4 Objectives

The literature review show that traces of inorganic salts in lignocellulosic biomass can produce significant effects on the thermal conversion of biomass. The aim of the present study is to enhance the current understanding of biomass ashes and their effect on biomass thermal conversion processes, particularly pyrolysis and gasification. To this end, the specific objectives are as follows:

- Perform proximate analysis to characterize wheat straw and select demineralization process;
- Evaluate possible physical and chemical changes to the wheat straw structure;
- Determine wheat straw ash content to evaluate ash thermal reactivity;
- Perform thermogravimetric experiments to investigate the impact of ashes on wheat straw pyrolysis;
- Perform gasification experiments to assess the impact of ashes on wheat straw gasification.

1.5 Thesis outline

This thesis is divided in five chapters. In the first chapter, the main motivations for this work are presented, as well as the general framework, a literature survey of previous studies and the specific objectives of the current study. The second chapter describes the experimental apparatus used and the methods applied in this experimental work. In the third chapter, the results are presented and discussed.

Chapters 1, 2 and 3 are divided in three main parts, according with the type of experiments carried out:

- Biomass characterization experiments,
- Pyrolysis experiments,
- Gasification experiments.

The chapters 4 and 5 present the conclusions and references for this work, respectively.

2. Materials and methods

2.1 Biomass characterization

The biomass chosen to perform this study was wheat straw and the particle size used was between 90 and 160 µm. For TGA experiments, raw, demineralized, and doped WS were used. For gasification, tests only raw and demineralized WS were used since only these could be obtained in sufficient quantity to perform the gasification tests. The samples were sieved using a SS-15 Gilson Economy 203 mm Sieve Shaker to the correct size and stored in sealed bags. Demineralized WS was obtained by demineralizing raw wheat straw. Water leaching [25] was chosen as demineralization procedure, as, according to literature, it reported good ash removal efficacy and preserved biomass chemical properties [29]. Process variations were tested to assess demineralization efficacy. Process efficacy was evaluated by comparing ash content of raw and demineralized samples on a dry basis, through proximate analysis. Final demineralization procedure was chosen to maximize ash content reduction. Doped WS was obtained by dry impregnation of raw WS with WS ashes (heated to 550 ºC).

Moisture was determined accordingly to standard *EN 14774-3* for solid biofuels. The analysis sample of solid biofuel is dried in a drying-oven (Figure 9) at a temperature of 105 ºC until constancy in mass is achieved – Figure 10 displays the equipment used for all weight measurements. Moisture content is then calculated from the loss of mass of the test sample. Constancy in mass is defined as a change not exceeding 1 mg in mass during a further period of heating at (105 ± 2) °C over a period of 60 minutes [42]. Moisture content was determined according to:

$$M = \frac{m_2 - m_3}{m_2 - m_1} \times 100 \quad (13)$$

where:

- m_1 is the mass, in g, of the empty crucible and lid;
- m_2 is the mass, in g, of the crucible and lid plus test sample before drying;
- m_3 is the mass, in g, of the crucible and lid plus test sample after drying.

Volatile matter was determined accordingly to standard *EN 15148:2009* for solid biofuels. A test portion of the general analysis sample was heated out of contact with ambient air at (900 ± 10) °C for 7 minutes. This is achieved by closing air intake of muffle furnace (Figure 11) and heating the sample in the crucible with the lid placed on top. The percentage of volatile matter is calculated from the loss in mass of the test portion after deducting the loss in mass due to moisture [43]. Volatile matter was thus determined according to:

$$VM = \frac{m_4 - m_5}{m_4 - m_1} \times 100 - M \quad (14)$$

where:

- m_1 is the mass, in g, of the empty crucible plus lid;
- m_4 is the mass, in g, of the crucible and lid plus test sample before heating;
- m_5 is the mass, in g, of the crucible and lid plus contents after heating;
- M is the moisture, as a percentage by mass, determined according to *EN 14774-3*.

Ash was determined according to standard *EN 18122* for solid biofuels. The ash content was determined by calculation from the mass of the residue remaining after the sample is heated in air under rigidly controlled conditions of time, sample weight and equipment specifications to a controlled temperature of (550 ± 10) °C [44]. The following heating routine was followed (heating performed with air intake opened and without crucible lid):

- Furnace temperature increased to 250 °C over a period of 30 minutes and maintained at this temperature for 60min to allow the volatiles to leave the sample before ignition.
- Furnace temperature increased to 550 °C over a period of 30 minutes and maintained at this temperature for 120 minutes. Reheated for further 30 minutes periods until the change in mass was lower than 0,5 mg.

Ash content is determined by:

$$ASH = \frac{m_8 - m_6}{m_7 - m_6} \times 100 \quad (15)$$

where:

- m_6 is the mass, in g, of the empty crucible;
- m_7 is the mass, in g, of the crucible plus the test sample before heating;
- m_8 is the mass, in g, of crucible plus remaining solid residue.

Fixed carbon was determined by difference.

For bulk density determination, a container of known volume, V_c, was weighed and subsequently tared. Biomass samples were then poured into the container from a constant height and levelled off. The mass of the biomass on was recorded on a precision scale as M_b. The bulk density, ρ_b, was calculated as follows:

$$\rho_b = \frac{M_b}{V_c} \quad (16)$$

FTIR analysis was performed on raw and demineralized WS samples with aid from a PerkinElmer Spectrum Two FT-IR Spectrometer (Figure 12). The infrared spectra of transmittance was recorded between 4000-650 cm^{-1} with a resolution of 2 cm^{-1}.

Chemical characterization of raw and demineralized WS was performed according to procedures reported by. For this, extractives, lignin, hemicellulose and cellulose were determined sequentially according to procedures reported by [45]–[47].

Extractives were determined by loading the boiling flask in the setup shown in Figure 13 sequentially with demineralized water, ethanol and hexane. Dried biomass was put inside the extraction chamber, inside an extraction thimble. Vapours from boiling flask condensed in the extraction chamber and removed extractives from biomass. Demineralized water was kept running for about 11 h, ethanol and hexane for 6 h. After all three solvents were used, biomass was removed, dried and weighed. The weight loss due to the use of solvents was attributed to the extractives [45].

Lignin content of biomass was determined by loading setup in Figure 14 with a predetermined quantity of dry extractive-free biomass, acetic acid, demineralized water and sodium chloride. For 6 h fresh portions of acetic acid and sodium chlorite were added each succeeding hour (at 70 ºC). The solution was then kept at 70 ºC for 24 h. At the end of reaction, the solution was washed with demineralized water and vacuum filtered. The remaining solids were oven dried for 20 h and weighed. The weight loss was attributed to lignin content [46].

Hemicellulose content of biomass was determined by loading setup in Figure 15 with a predetermined quantity of dry extractive and lignin-free biomass and 150 mL of sodium hydroxide (NaOH) solution (0.5 mol/l). The solution was kept at 80 ºC for 3.5 h and was later washed with demineralized water and vacuum filtered. The remaining solids were oven dried for 20 h and weighed. The weight loss was attributed to hemicellulose content [47]. Cellulose was determined by difference.

Figure 9. Drying Oven.

Figure 10. Precision Scale.

Figure 11. Muffle Furnace

Figure 12. PerkinElmer Spectrum Two FT-IR Spectrometer

.

Figure 13. Setup for extractive determination.

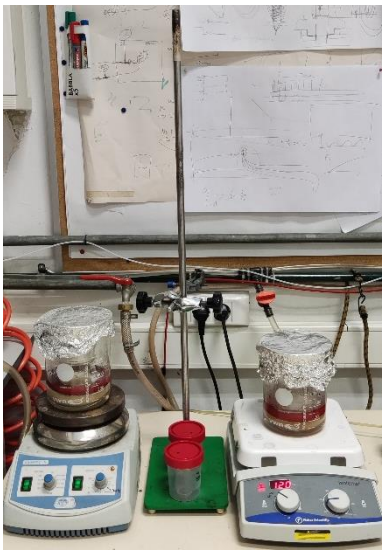

Figure 14. Setup for lignin and hemicellulose determination.

2.2 Pyrolysis experiments

2.2.1 Experiment setup

The pyrolysis study of raw, demineralized WS and doped WS was carried out by Horizontal Differential Thermogravimetry in a model 7200 Simultaneous Thermal Analyzer of the Hitachi brand (Figure 15). A scheme of the main components of this equipment are presented in Figure 16.

Figure 15. Model 7200 Simultaneous Thermal Analyzer.

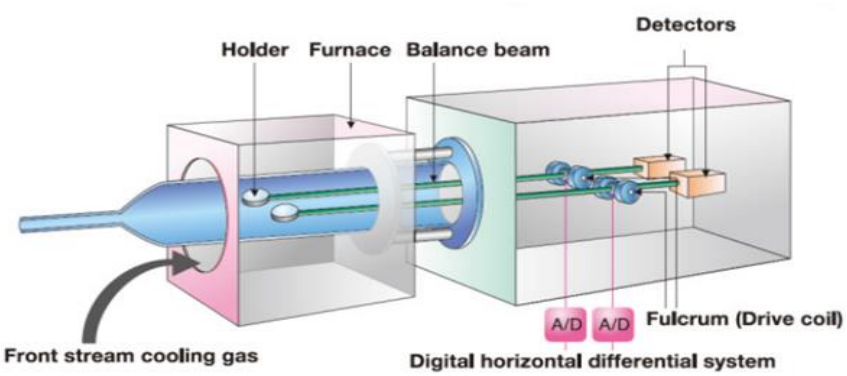

Figure 16. Main components of a Horizontal Differential Thermal Analyzer.

2.2.2 Experimental procedure

Equipment was turned on and desired test parameters were registered in the software. Furnace cover was opened to expose two beams supported by a precision balance. Two pans - one with the sample material and one empty - were placed on the holders, at the end of the beams. Once the weight values stabilized, they were recorded, and the cover was closed. Nitrogen was then opened, and testing was initiated. The information regarding the temperature and mass variations was sent to a computer to process the data in the form of thermogravimetric (TG) and differential thermogravimetric (DTG) curves.

2.2.3 Parameters

The thermogravimetric study of raw, demineralized, and doped WS was carried out with the parameters presented in Table 2.

Table 2. TGA experiment parameters

Biomass	Sample Size (mg)	Initial Temperature (ºC)	Final Temperature (ºC)	Heating Rate (ºC/min)	Nitrogen flow rate (mL/min)
Raw WS	5.5	30	900	5	100
Demineralized WS	3.1				
Doped WS	6.6				

2.2.4 Data post-processing

During the TGA, at any given time the total mass of the sample can be defined as $m(t) = m_r(t) + m_f$, where $m_r(t)$ and m_f are the reactive and nonreactive parts – the ashes – of the total mass. Additionally, m_d can be defined as the sample´s total dry mass (taken at $\sim 140\,ºC$). Based on these definitions, a fraction of biomass decomposition may be written in nondimensional form as $\alpha(t) = 1 - \frac{m(t)-m_f}{m_d-m_f}$. This approach is intended to assess the influence of the non-reactive part of biomass more clearly on the reactive portion. TG and DTG curves presented will therefore refer to the normalized mass and the normalized mass loss rate: $(1-\alpha)$ and $\frac{d(1-\alpha)}{dt}$, respectively. Also, before any post-processing analysis of these measurements, the raw TGA data was smoothed out using a moving average method to reduce the noise (Figure 17), without compromising the accuracy of the measurements.

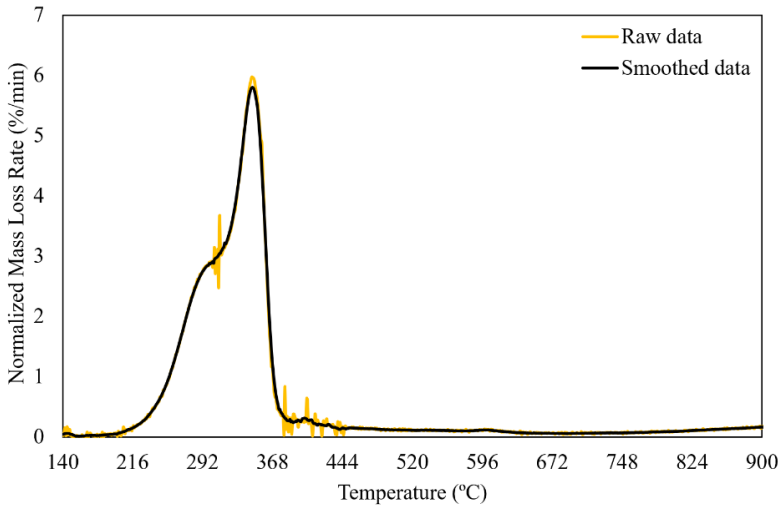

Figure 17. Raw and smoothed TGA data.

2.3 Gasification experiments

2.3.1 Experimental setup

The gasification experiments were carried out in the drop tube gasification system (Figure 18). This system is comprised of a drop tube furnace (DTF), a fuel feeding system, gas supply system, a particle sampling system, a tar collecting system and a gas sampling and analysis system.

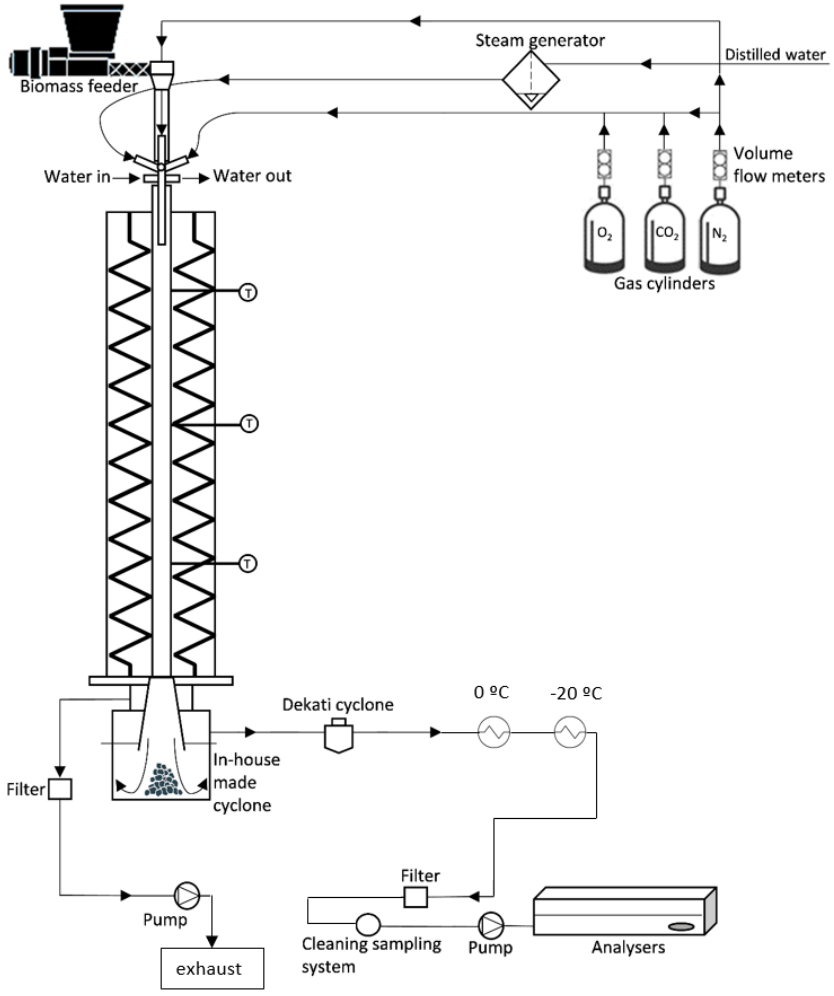

Figure 18. Drop Tube Gasification System.

The fuel feeding system consists of a collecting bowl, twin-screw volumetric feeder, mixing box and injector. The pulverized biomass is poured onto the collecting bowl and through the action of the screw feeder is forced to move towards the mixing box at a controlled rate, where it mixes with the transport gas, N_2. Through the water-cooled injector, the biomass and transport fluid are then fed into the gasification reactor at a controlled rate and experience various temperatures and atmosphere conditions depending on the test setup. The gas supply system uses bottled gases as source for O_2, N_2 and CO_2 gases and volumetric flow meters to control the amount of gas supplied. When steam is used, a separate steam generator is required which generates steam from distilled water. The desired gas is

then introduced into the reactor through a concentric passage inside the injector. The solid particle sampling system is composed of two cyclones (commercial cyclone and in-house cyclone) that aim to collect larger particles (>10μm). The Dekati cyclone is fitted with an external heating blanket to avoid condensation of undesirable substances. The tar collecting system consists of 4 collecting bottles and cooling equipment. The first 2 bottles are kept at 0 ºC and the other two at -20 ºC. The first and last bottles are not filled with isopropanol, whereas the second and third bottles are filled with 50mL and 100mL, respectfully. This helps capture the tars in the isopropanol. The gas sampling and analysis system includes a gas cleaning apparatus (to ensure that any particles remaining in the gas flow are captured), gas analysers and a pump to ensure correct flow rate for analysers. Gas composition in terms of O_2, CO_2 and CO volume percentage is directly given by analysers during experiments. Gas samples can also be collected with sampling bags and posteriorly analysed with the help of a gas chromatograph, which gives the remaining gases´ volume percentage in the product gas.

2.3.2 Experimental procedure

Before testing was initiated, the water circuit was opened to ensure proper cooling of the injector. Temperature was initially set for 400 ºC, after which, temperature increments of 200 ºC were used with at least 5 minutes stabilization period (to ensure proper heating and equipment safety) until test temperature was reached. For correct test starting conditions (with no delay), the mixing box had to be packed with biomass. To ensure this, approximately 100 g of previously dried biomass were put in the collecting bowl and screw feeder was turned on, with mixing box disconnected from DTF. When the mixing box was filled, the screw feeder was turned off, excess biomass was collected and put back in the collecting bowl and mixing box was reconnected with DTF. To reduce exposure time of dry biomass to the surrounding atmosphere the DTF heating procedure was done in parallel with mixing box filling procedure. When the desired temperature was reached, the N_2 bottle was opened to the desired amount and O_2 levels were checked in the O_2 analyser. After O_2 levels dropped below 0.2%, the desired gasification atmosphere was introduced. Once levels of O_2 reached a final steady state, the screw feeder was set to a specified rate and testing was initiated.

Each test had a duration of 30 minutes. O_2, CO_2 and CO volume fractions were monitored and recorded during the full duration of the test. These measurements were manually acquired approximately each minute. Each recorded value was a computer average of a 30 second period, in which several measurements were automatically taken each second. Gas samples were taken approximately halfway through the test for subsequent analysis. Solid particles were collected for the full duration of the test. To end the test, all gas bottles in use were closed and the screw feeder was turned off.

After the test ended, the temperature was either maintained/increased if additional tests were to be performed or else decreased to ambient temperature. Cyclones were removed and solid particles collected. Collecting bottles were removed and their contents stored. Sampling bags were analysed in a Clarus 500 Gas Chromatograph.

2.3.3 Parameters

The gasification study of raw and demineralized WS was carried out with the parameters presented in Table 3.

Table 3. Gasification experiment parameters

Biomass	**Temperature (°C)**	**Biomass flow rate (g/h)**	λ	**Particle diameter (μm)**	**Nitrogen flow rate (L/min)**
Raw WS	900	24	0.4	90-160	9.9
	1000				
	1100				
	1200				
Demineralized WS	900	15	0.4	90-160	9.9
	1000				
	1100				
	1200				

3. Results and discussion

3.1 Biomass characterization

Demineralization procedures consisted mainly of four steps: sample and solution preparation, stirring, filtration and washing and, finally, drying. Tested variations included changes to leaching time and water/biomass ratio. Although higher leaching temperatures and use of acidic solvents like HCl are known to increase ash removal, they also reportedly change the chemical composition of biomass and therefore were not considered in this work. Table 4 presents the various demineralization processes tested and their respective results in terms of relative ash reduction.

Table 4. Demineralization process variations and results

Demineralization Process	Leaching Time (h)	Temperature (ºC)	Water/Biomass Ratio (mL/g)	Ash Relative Variation (wt. % db)
A	1	30	1:20	-30.6
B	1	30	1:40	-31.9
C	24	30	1:20	-59.9
D	24	30	1:40	-58.9

From Table 4 we can initially infer that water/biomass ratio of 1:20 is near the solubility limit since increase of this ratio to 1:40 resulted in a very small improvement in ash removal (4%) from procedure A to B and even worsened from case C to D (-1.7%). The same cannot be said about leaching time, as an increase of 23h resulted in a significant improvement in both cases: 95.8% from A to C and 84.6% from B to D. Moisture content of WS samples was 9.6% for raw WS and 10.5%,10.1%,10.3% and 10.8% for straw obtained by deashing processes A through C, respectfully.

Figure 19 shows the results of the proximate analysis of raw WS and demineralized WS samples on a dry basis. It reveals that besides an evident reduction in ashes, demineralized WS has a significantly higher yield of volatile matter and decrease of the amount of fixed carbon. Careful inspection of the resulting demineralized biomass samples show that it is significantly less dense than raw wheat straw (see Table 5). Demineralization process C was chosen as it was the process with the highest ash removal efficacy and allowed for the highest yield of demineralized biomass as a result of a lower water/biomass ratio.

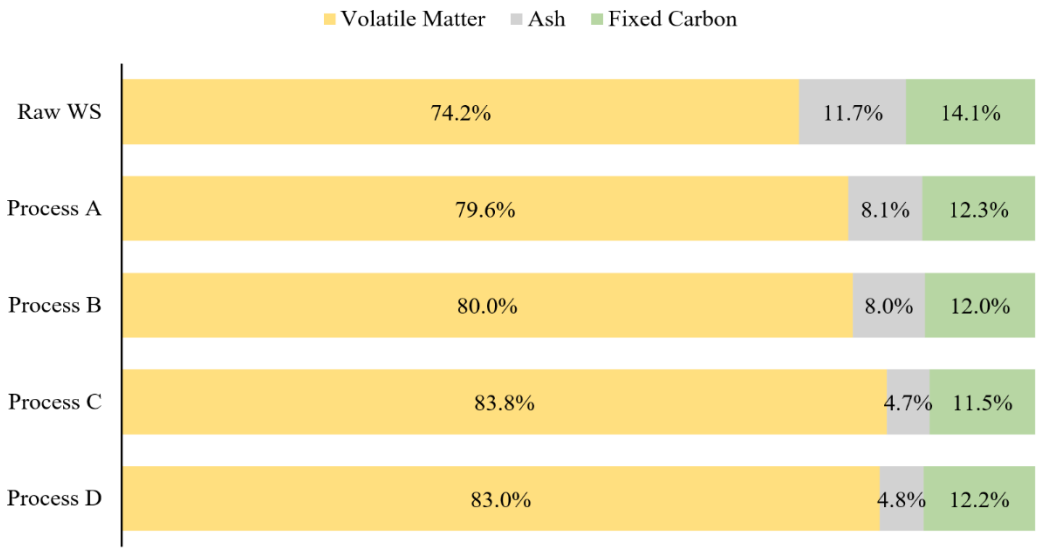

Figure 19. Proximate Analysis of Raw and Demineralized WS samples (wt. % dry basis)

Table 5. Raw and demineralized WS bulk density

Biomass	**Oven-Dry Bulk Density (kg/m3)**
Raw WS	393.1 ± 10
Demineralized WS	153.6 ± 6

To evaluate possible chemical changes in the demineralized WS, FTIR spectroscopy was employed. This is a reliable technique that can be used to determine the effect of pre-treatment of biomass. However, it essentially provides qualitative structural information rather than quantitative information.

Figure 20 presents the resulting IR spectra of raw and demineralized WS samples in terms of transmittance percentage and Table 6 shows the wavenumber of the major transmittance bands present in said spectra. We can see that the characteristic spectra of raw and demineralized WS are very closely aligned, being almost coincident in terms of peak location and with very similar peak intensities. Since no major changes can be noticed in the characteristic pattern of transmittance, from a qualitative point of view, we can say that demineralization procedure did not have a major impact on the chemical composition of WS.

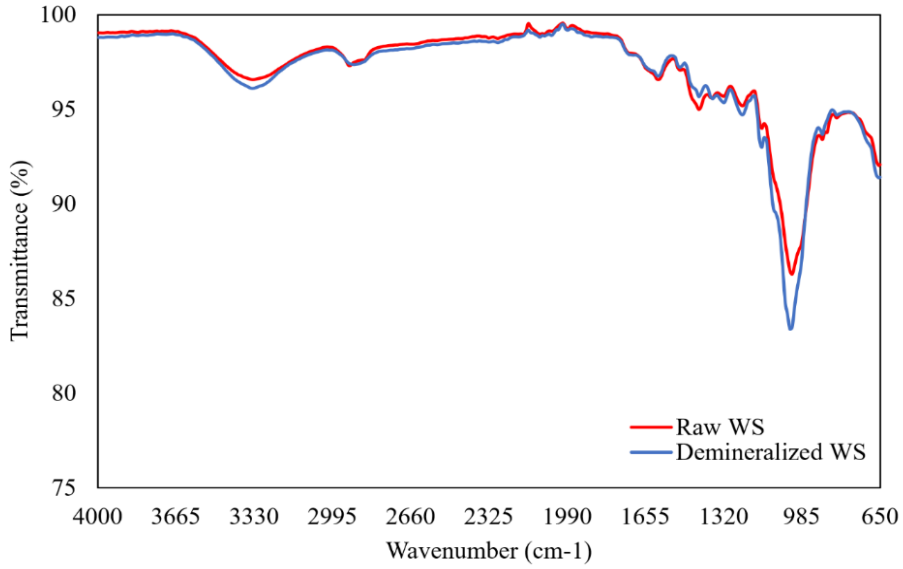

Figure 20. IR spectra of Raw and Demineralized WS

Table 6. Major transmittance bands in IR spectra of WS samples

Sample	Wavenumber of major transmittance bands (cm^{-1})								
Raw WS	3336	2924	1604	1424	1240	1160	1028	896	658
Demineralized WS	3342	2906	1602	1426	1240	1162	1032	896	662

Chemical characterization was performed to further assess chemical composition of WS samples. Table 7 compiles the main results of this characterization. Firstly, we can see that there is a 7.3 wt. % db difference in extractives, between raw and demineralized WS. Considering that, from proximate analysis, it was concluded that an absolute reduction of about 7 wt. % db was achieved in ash content, this reduction in extractives can be attributed to the deashing pre-treatment.

Table 7. Chemical composition of WS samples and typical literature values [48]

Sample	Lignin (wt. % daf)	Hemicellulose (wt. % daf)	Cellulose (wt. % daf)	Extractives (wt. % db)
Raw WS	46.2	11.5	42.3	17.7
Demineralized WS	43.9	10.6	45.5	10.4
Literature	18 - 30	18 - 35	29 - 43	-

Table 7 also contains data regarding the structural components of WS. Looking at the obtained values we can observe that lignin content is slightly overestimated and hemicellulose content is underestimated, when comparing to the typical values found in the literature for this type of biomass. This might be explained by the fact that during the delignification process application of excess sodium chlorite will remove lignin but hemicellulose could also be lost [46]. Similarly, higher temperatures and longer reactions times will also augment delignification reaction and result in the loss of some hemicellulose. In the lignin determination, during the 24 h period, some water in the bath solution was lost and as a consequence overall temperature was increased by about 5-10 ºC, thus explaining the excessive weight loss attributed to the lignin content and consequent inadequate weight loss attributed to hemicellulose. However, sum of hemicellulose and lignin is consistent with literature, hence why cellulose – being determined by difference - remained unaffected. Nevertheless, relative changes in lignin, hemicellulose and cellulose between raw and demineralized WS were about 5%, 8% and 8%, respectively. Since the result bias is consistent for both samples and relative changes are not significant, we can still conclude that no major chemical changes occurred from the deashing pre-treatment of raw WS.

To help understand the thermal stability of ash forming elements, ashes were determined following the procedure described in section 3.1 for ash determination, using increasingly higher temperatures for the final stage. Figure 21 compiles the results of these experiments. Figure 22 shows WS ashes determined at the lowest/highest temperatures for both raw and demineralized samples. It was found that ashes determined at 650 ºC were 8% and 9.3% lower than those determined at 550 ºC, for raw WS and demineralized WS, respectively. As for ashes determined at 1050 ºC, these were 15.6% lower for raw WS and about 18% lower for demineralized WS. We can also see that reduction in ashes is higher for demineralized WS for all temperatures except 650 ºC. This might indicate that ashes removed with demineralization procedure were mostly components that easily degrade with temperature. These results are consistent with findings from previous studies. Vassilev et al. [14] revealed that biomass ashes determined at 1100 ºC could be 7 to 59% lower than those determined at 500 ºC, with minimum losses occurring for the biomass varieties highly enriched in silica and silicates, and maximum losses occurring for biomass varieties abundant in Ca, Cl, Fe, K, Mg, Na, P, S, chlorides, sulphates, carbonates and phosphates. Also, ashes determined at 1050 ºC (high temperature ashes) presented a different behaviour that those determined at 550 ºC (low temperature ashes): LTA could be easily removed from the ceramic crucible whereas HTA could not be entirely removed due to some ash melting taking place at these higher temperatures. This is expected since Vassilev et al. showed that initial deformation of wheat straw ashes could be as low as 915 ºC [14]. These results show that, in fact, ashes are not entirely inert, as some elements react and thermally degrade at higher temperatures.

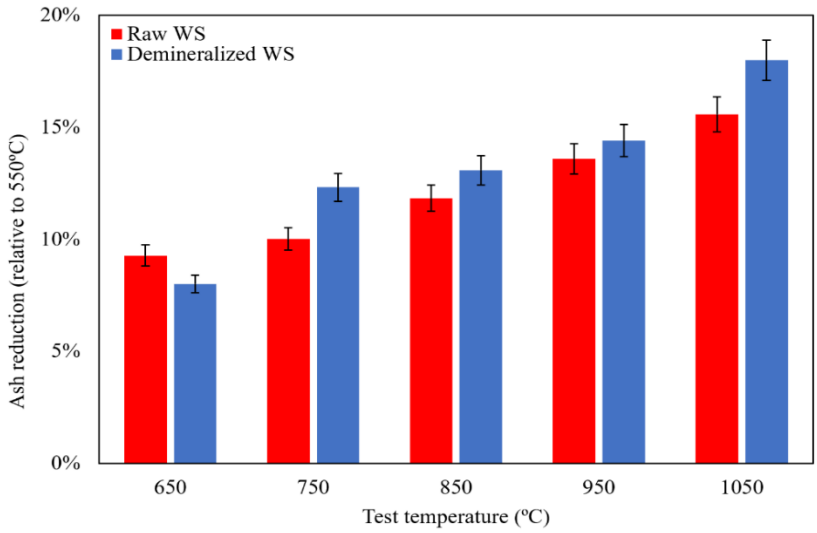

Figure 21. Raw and demineralized ash reduction relative to ashes determined at 550ºC

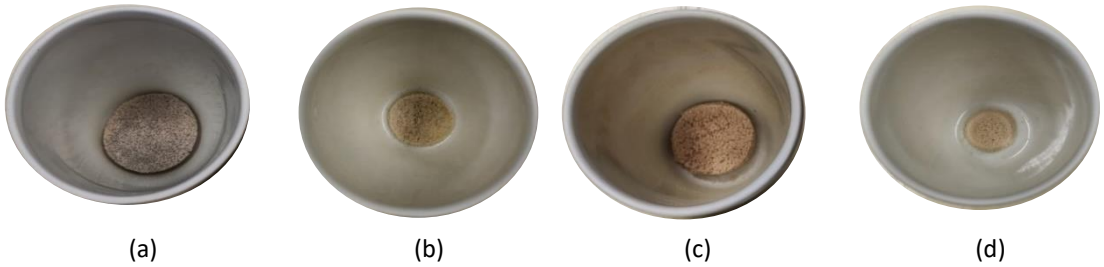

Figure 22. Raw WS ashes determined at (a) 550 ºC, (b) 1050 ºC and Demineralized WS ashes determined at (c) 550 ºC and (d) 1050 ºC.

3.2 Pyrolysis experiments

The pyrolysis study of raw, demineralized WS and doped WS was carried out by horizontal differential thermogravimetry. TG and DTG curves were obtained in the temperature range between 30 °C and 900 °C, in a model STA 7200 of the Hitachi brand, under atmosphere of nitrogen with 100 mL/min purge rate, heating rate of 5 °C/min and using a platinum crucible containing approximately 5 mg of test sample for raw WS, 3 mg for demineralized WS and 6mg for doped WS. Since the objective of this work does not consider the study of the drying process and it makes use of biomasses with varying degrees of ash content, the TGA results that will be presented in this section will be normalized as described in section 2.2.4. Also, only the temperature interval significant for pyrolysis is shown (140 ºC < T < 900 ºC). Figure 23 shows the resulting TG and DTG curves obtained from the thermogravimetric analysis of WS samples.

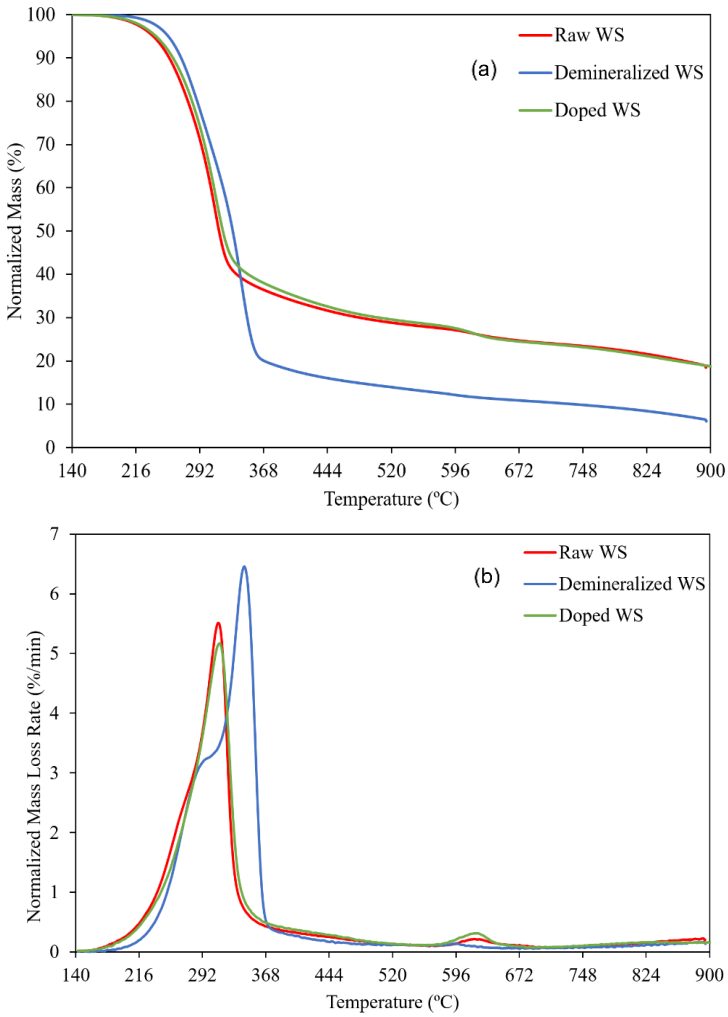

Figure 23. Resulting TG (a) and DTG (b) curves of TGA of WS samples.

The resulting TG (Figure 23 (a)) curves represent a typical TG curve. Initial drying phase is not shown, the middle part of the curves is characterized by the intensive process of volatile extraction (200 ºC < T < 370 ºC), which results in a steeper curve of mass change and the final part presents a much more levelled mass loss up until the final temperature of 900 ºC. The initial and final temperatures of primary decomposition are both defined as the temperature where the rate of weight loss is 0.5 wt.%/min [30].

After the normalization process, the TG curves, raw and doped WS mostly collapse into a single curve meaning that at first glance dry impregnation of raw WS with WS ashes did not produce any major effects. Table 8 presents the main results from the TG and DTG curves: initial, peak, and final temperatures of the primary decomposition - T_i, T_{peak} and T_f –, the final sample mass - TG_{end} and the largest value of mass loss rate recorded - DTG_{peak}. From this Table, we can observe that initial, peak, and final temperatures of the primary decomposition of raw and doped WS are very similar, confirming that dry addition of WS ashes did not influence the pyrolysis behaviour of WS. Demineralized WS, however, appears to thermally degrade at higher temperatures and to a higher extent than raw and

doped WS samples. Table 8 shows that initial, peak and final decomposition temperatures of demineralized WS were respectively 19 ºC, 31 ºC, and 12 ºC higher than raw WS. Also, normalized mass losses of raw and doped WS at 900 ºC are near identical at 18.4% and 18.3%, whereas for demineralized straw is considerably lower at 6%. Previous studies found that catalysed pyrolysis increased the char yields significantly [34].

In both raw and doped WS, DTG curves (Figure 23 (b)) present a broad and featureless peak with similar values at near identical temperatures - DTG_{peak}. Hemicellulose and cellulose are associated with the peak of the DTG curves, meaning that the rate curves of these two components overlap each other during their decomposition process. In demineralized WS a different trend can be observed. Besides having a higher peak than raw and doped WS, there appears to be a shift of the peak of the DTG curve towards a higher temperature as well as the appearance of a ”shoulder” near the same decomposition temperature as the raw and doped WS peaks. This phenomenon was observed by Jensen et al. [30] and he argued that the washing of the straw cause the splitting of the main DTG peak into the low-temperature peak- which was due to the decomposition of hemicellulose -, and the high-temperature peak - which was associated with cellulose decomposition. In fact, the shoulder and peak decomposition temperatures of the demineralized WS – 310 ºC and 340 ºC – suggest that their overlapping decomposition was partially split by the demineralization process, since these temperatures are consistent with the hemicellulose and cellulose characteristic decomposition temperatures reported in literature.

Table 8. Main results of TGA of WS samples

Sample	T_i **(ºC)**	T_{peak} **(ºC)**	T_f **(ºC)**	DTG_{peak} **(%/min)**	TG_{end} **(%)**
Raw WS	217	311	357	5.5	18.4
Doped WS	218	312	365	5.2	18.3
Demineralized WS	236	342	369	6.5	6.0

Major volatile extraction happens roughly between 200 ºC and 370 ºC for all samples, with primary pyrolysis taking place up until ~ 600 ºC. At roughly 620 ºC, a smaller peak can be seen in the DTG curves of raw and doped WS. This mass loss rate peak appears to increase in order of increasing ash content and is not present in the demineralized WS curve. Similar findings were reported by Han et al. [32]. A second decomposition stage near 600 ºC was found to increase with increasing amount of CaO - a common compound in biomass ashes. This increase was attributed to the thermal degradation of carbonates in the ashes. This peak can, thus, be attributed to the thermal degradation of some elements in the ashes, as the temperature range of the second stage is typical of the degradation of some carbonates [49]. Like previously mentioned ashes are in fact, to some degree, reactive and at higher temperatures this becomes more evident.

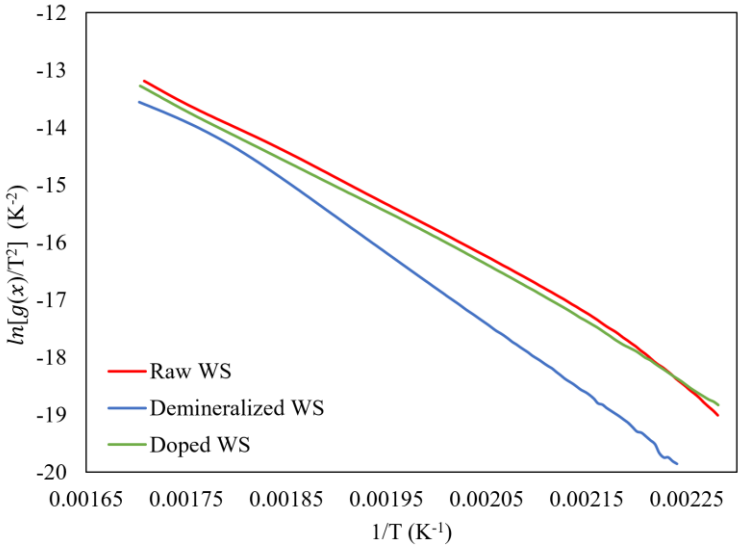

Figure 24. Kinetic analysis of WS samples

Table 9. Apparent first order kinetic parameters of WS pyrolysis

Raw WS	$E_a\ (kJ/mol)$	79.7
	$k_0\ (s^{-1})$	0.0216
	R^2	0.995
Doped WS	$E_a\ (kJ/mol)$	79.0
	$k_0\ (s^{-1})$	0.0175
	R^2	0.995
Demineralized WS	$E_a\ (kJ/mol)$	99.4
	$k_0\ (s^{-1})$	1.2
	R^2	0.998

In the present study, the first reaction order mechanism ($n = 1$) was used since it is the most common one used to describe the biomass thermal decomposition. Following the Coats-Redfern (CR) method mentioned in section 1.2.4., Figure 24 shows the resulting plot of $\ln\left[\frac{g(\alpha)}{T^2}\right]$ vs $\frac{1}{T}$ from which the apparent kinetic parameters can be obtained. Table 9 presents these parameters for all WS samples as well as the coefficient of determination of the linear fittings. From this table, it can be noticed that the activation energy of raw and doped straw is very similar at 79.7 kJ/mol and 79 kJ/mol, respectively, whereas demineralized straw clearly suffers an increase to 99.4 kJ/mol. This result is coherent with previous findings that have shown catalysed pyrolysis of biomass lowered the average apparent first order activation energy for pyrolysis by up to 50 kJ/mol [34].

It is important to remember that lower activation energy implies that the reaction needs less energy from the surroundings. Reactions with high activation energy need high temperature or long reaction time. However, if a catalyst is added to the reaction, the activation energy is lowered and the

reaction proceeds faster, increasing the rate constant. Catalysts not only reduce the energy barrier, but can also induce completely different reaction pathways [22]. Thus, we can conclude that in fact, the demineralization process removed some elements which may have benefited the pyrolysis of wheat straw, since removing these elements resulted in a change in the reaction pathway of the primary decomposition: the one-step decomposition of wheat straw (where cellulose and hemicellulose decomposition overlap) was divided into a 2-step process with higher energy requirements.

3.3 Gasification experiments

The gasification tests were performed in the drop tube gasification system. This system uses an entrained-flow type of gasifier, where the gasifying atmosphere is responsible for transporting the fuel particles through the reactor. As result, the producer gas obtained was mainly formed by N_2 (~98 vol.%). Figure 26 shows the evolution of the producer gas composition as a function of the operating temperature. It contains the normalization of the main produced gases: CO, CO_2, CH_4 and H_2.

For the operating temperature between 900 and 1200 °C, the H_2 yield significantly increased from 7.8 vol % to 26.3 vol % for demineralized WS and from 7.3 vol % to 30.3 vol % for raw WS. The CO yield slightly increased from 48.6 vol.% to 51.4 vol % for demineralized straw but slightly decreased for raw straw, from 51.6 vol % to 44.6 vol %. CO_2 yield decreased in both straws significantly: 28.7 vol% to 19.5 vol % and 37.2 vol% to 17.6 vol %, for raw and demineralized samples, respectively. Finally, CH_4 yields decreased from 12.4 vol % to 5.6 vol % for raw WS and from 6.4 vol % to 4.7 vol %. Besides the CO reduction observed in raw straw - which could not be explained - these trends are well understood. Previous studies [35] had established that increasing operating temperatures promotes endothermic reactions. While the temperature increases, it promotes the reactions R1, R2 and R3 (see Table 1). The Boudouard reaction (R1, Table 1) produces CO consuming CO_2; the Water-Gas (R2, Table 1) and Methane Steam Reforming (R13, Table 1) reactions consume H_2O and CH_4 producing CO and H_2. This explains the global decrease in the CO_2 and CH_4 yields, and the increase in the H_2 and CO yields.

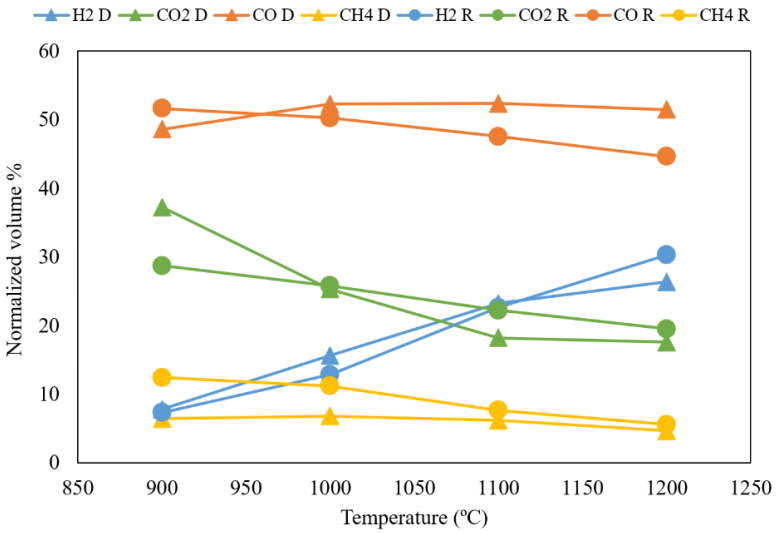

Figure 25. Normalized syngas composition for different operating temperature.

Figure 26 shows the normalized values of the solid yield – without ashes – for different operating temperatures. These values refer to the solid yield without ashes and are normalized by the biomass input. Raw WS normalized solid yield was reduced from 8.2 wt.% at 900 ºC to 4 wt.% at 1200 ºC whereas demineralized straw had 7 wt.% solid yield at 900 ºC and 4.3 wt.% at 1200 ºC. Results show a clear tendency of solid yield decrease with increasing temperatures, as reported by previous studies [35], [38].

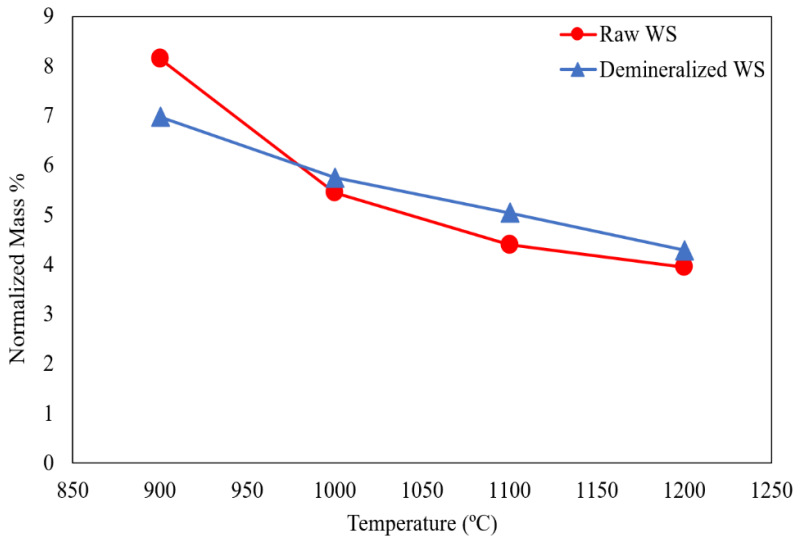

Figure 26. Normalized solid carbon yield for different operating temperatures

Although syngas composition and solid yield evolution with operating temperature are mostly in accordance with previous findings no clear effect of biomass ashes could be observed. It was established from previous studies that biomass with higher quantities of ashes is expected to have a larger reactivity and to benefit from catalysed heterogeneous char gasification reactions, leading to lower soot yields and favouring the presence of lighter gas species [37], [41]. In the present study none of the aforementioned results could be reproduced. This could be related to:

- Quantity of removed elements – quantity of removed elements could be insufficient to have any noticeable difference in gasification behaviour.
- Type of elements removed – not all ash forming elements are responsible for catalytic effects.
- Influence of physicochemical changes in the demineralized biomass – i.e. change of biomass density.

4.Conclusions

4.1 Work Summary

The proposed objectives were mostly achieved. Demineralization process was successful in removing ash forming elements from wheat straw without affecting its chemical structure. Some insight into ash thermal stability was gathered. The effect of WS ashes on pyrolysis behaviour of wheat straw was studied by thermogravimetry - using raw, doped and demineralized WS. Although, effect of WS ashes on gasification were inconclusive, the resulting temperature trends were generally in accordance with previous studies.

4.2 Main conclusions

The main conclusions of this work are as follows:

1. Demineralization of wheat straw using deionized water resulted in the removal of about 7 wt. % db of ash content of wheat straw.
2. Shifting of peaks of demineralized sample towards high temperature in TG and DTG curves showed that demineralized sample was more resistant towards thermal degradation.
3. Demineralization of wheat straw resulted in the partial split of the thermal decomposition of hemicellulose and cellulose and the overall increase of the energy required to thermally degrade wheat straw.
4. Dry addition of WS ashes did not lead to the formation of chemical bounds between inorganic salts and the organic phase, and therefore did not influence pyrolysis behaviour of wheat straw.

4.3 Recommendations for future work

As future work it would be interesting to explore different ash doping techniques, since dry addition did not produce any relevant results. Also, it would be interesting to study the influence of individual ash components on pyrolysis of biomass.

Regarding the gasification experiments additional experiments should be performed. In the present study chemical properties remained the same but physical changes were introduced to the wheat straw, which may have caused problems with biomass feeding to the reactor. Additional demineralization processes should be investigated to maximize ash removal without compromising biomass physical and chemical properties. Also, specific ash inorganic components should be evaluated in order to more accurately predict gasification behaviour changes.

5.References

[1] UNDESA, *World Urbanization Prospects*, vol. 12. 2018.

[2] U. S. E. I. Energy Information Administration, “International Energy Outlook 2019,” *U.S. Energy Inf. Adm.*, vol. September, no. 09, pp. 25–150, 2019.

[3] R. M. Goss, “BP Statistical Review of World Energy 2019 | 68th edition,” 2019.

[4] J. G. J. Olivier and J. A. H. W. Peters, “Trends in Global CO2 and Total Greenhouse Gas Emissions:Report 2019. PBL Netherlands Environmental Assessment Agency The Hague,” vol. 2020, no. 4068, p. 70, 2020, [Online]. Available: www.pbl.nl/en.

[5] M. T. Masson-Delmotte, V., P. Zhai, H.-O. Pörtner, D. Roberts, J. Skea, P.R. Shukla, A. Pirani, W. Moufouma-Okia, C. Péan, R. Pidcock, S. Connors, J.B.R. Matthews, Y. Chen, X. Zhou, M.I. Gomis, E. Lonnoy, T. Maycock and T. Waterfield, “Summary for Policymakers. In: Global Warming of 1.5°C. An IPCC Special Report on the impacts of global warming of 1.5°C above pre-industrial levels and related global greenhouse gas emission pathways, in the context of strengthening the global response to,” *One Earth*, vol. 1, no. 3, pp. 374–381, 2019, doi: 10.1016/j.oneear.2019.10.025.

[6] B. Looney, “Statistical Review of World Energy, 2020 | 69th Edition,” *Bp*, vol. 69, p. 66, 2020, [Online]. Available: https://www.bp.com/content/dam/bp/business-sites/en/global/corporate/pdfs/energy-economics/statistical-review/bp-stats-review-2020-full-report.pdf.

[7] Basu, P. (2010) Biomass Gasification and Pyrolysis, Piratical Design and Theory. Elsevier.

[8] C. Harvey and N. Heikkinen, “Congress Says Biomass Is Carbon-Neutral, but Scientists Disagree,” *E&E News*, 2018. https://www.scientificamerican.com/article/congress-says-biomass-is-carbon-neutral-but-scientists-disagree/.

[9] S. V. Vassilev, D. Baxter, L. K. Andersen, and C. G. Vassileva, “An overview of the chemical composition of biomass,” *Fuel*, vol. 89, no. 5, pp. 913–933, 2010, doi: 10.1016/j.fuel.2009.10.022.

[10] D. Sietske Boschma, I. Kees, and W. Kwant, “Netherlands Programmes Sustainable Biomass,” *NL Agency Minist. Econ. Aff.*, no. June, pp. 6–30, 2013, [Online]. Available: http://english.rvo.nl/sites/default/files/2013/12/Straw report AgNL June 2013.pdf%0Awww.wageningenur.nl/fbr.

[11] A. M. Mansor, J. S. Lim, F. N. Ani, H. Hashim, and W. S. Ho, “Characteristics of cellulose, hemicellulose and lignin of MD2 pineapple biomass,” *Chem. Eng. Trans.*, vol. 72, no. March 2018, pp. 79–84, 2019, doi: 10.3303/CET1972014.

[12] L. J. Gibson, “The hierarchical structure and mechanics of plant materials,” *J. R. Soc. Interface*, vol. 9, no. 76, pp. 2749–2766, 2012, doi: 10.1098/rsif.2012.0341.

[13] C. G. Vassileva and S. V. Vassilev, “Behaviour of inorganic matter during heating of Bulgarian coals: 1. Lignites,” *Fuel Process. Technol.*, vol. 86, no. 12–13, pp. 1297–1333, 2005, doi: 10.1016/j.fuproc.2005.01.024.

[14] S. V. Vassilev, D. Baxter, L. K. Andersen, and C. G. Vassileva, “An overview of the composition and application of biomass ash. Part 1. Phase-mineral and chemical composition and classification,” *Fuel*, vol. 105, pp. 40–76, 2013, doi: 10.1016/j.fuel.2012.09.041.

[15] G. Zając, J. Szyszlak-Bargłowicz, W. Gołębiowski, and M. Szczepanik, “Chemical characteristics of biomass ashes,” *Energies*, vol. 11, no. 11, pp. 1–15, 2018, doi: 10.3390/en11112885.

[16] A. Molino, S. Chianese, and D. Musmarra, “Biomass gasification technology: The state of the art overview,” *J. Energy Chem.*, vol. 25, no. 1, pp. 10–25, 2016, doi: 10.1016/j.jechem.2015.11.005.

[17] “Propanal.” https://webbook.nist.gov/cgi/cbook.cgi?ID=C123386&Mask=80 (accessed Jul. 22, 2021).

[18] Derrick, Michele R., Dusan Stulik, and James M. Landry. 1999. Infrared Spectroscopy in Conservation Science. Scientific Tools for Conservation. Los Angeles, CA: Getty Conservation Institute. http://hdl.handle.net/10020/gci_pubs/infrared_spectroscopy

[19] M. BREBU and C. VASILE, “THERMAL DEGRADATION OF LIGNIN – A REVIEW,” 2009, doi: 10.1016/j.wasman.2015.11.041.

[20] B. B. Uzun, E. Apaydın Varol, J. Liu, and V. J. Bruckman, Eds., “Biochar Production,” in *Biochar: A Regional Supply Chain Approach in View of Climate Change Mitigation*, Cambridge: Cambridge University Press, 2016, pp. 197–288.

[21] S. S. M. Mostafa and N. S. El-Gendy, “Evaluation of fuel properties for microalgae Spirulina platensis bio-diesel and its blends with Egyptian petro-diesel,” *Arab. J. Chem.*, vol. 10, pp. S2040–S2050, 2017, doi: 10.1016/j.arabjc.2013.07.034.

[22] “The Arrhenius Law - Activation Energies.” Jun. 28, 2020, [Online]. Available: https://chem.libretexts.org/@go/page/1444.

[23] D. López-González, M. Fernandez-Lopez, J. L. Valverde, and L. Sanchez-Silva, “Thermogravimetric-mass spectrometric analysis on combustion of lignocellulosic biomass,” *Bioresour. Technol.*, vol. 143, pp. 562–574, 2013, doi: 10.1016/j.biortech.2013.06.052.

[24] “All Power Labs.” https://www.allpowerlabs.com/gasification-explained (accessed Jul. 22, 2021).

[25] P. Das, A. Ganesh, and P. Wangikar, “Influence of pretreatment for deashing of sugarcane bagasse on pyrolysis products,” *Biomass and Bioenergy*, vol. 27, no. 5, pp. 445–457, 2004, doi: 10.1016/j.biombioe.2004.04.002.

[26] M. Asadieraghi and W. M. A. Wan Daud, “Characterization of lignocellulosic biomass thermal degradation and physiochemical structure: Effects of demineralization by diverse acid solutions,” *Energy Convers. Manag.*, vol. 82, pp. 71–82, 2014, doi: 10.1016/j.enconman.2014.03.007.

[27] L. Jiang, S. Hu, L. Sun, S. Su, K Xu , L. He, J. Xiang, “Influence of different demineralization treatments on physicochemical structure and thermal degradation of biomass,” *Bioresour. Technol.*, vol. 146, pp. 254–260, 2013, doi: 10.1016/j.biortech.2013.07.063.

[28] D. Mourant, Z. Wang, M. H, X. S. Wang, M. G. Perez,K. Ling, C. Z. Li, “Mallee wood fast pyrolysis: Effects of alkali and alkaline earth metallic species on the yield and composition of bio-oil,” *Fuel*, vol. 90, no. 9, pp. 2915–2922, 2011, doi: 10.1016/j.fuel.2011.04.033.

[29] B. M. Jenkins, R. R. Bakker, and J. B. Wei, “On the properties of washed straw,” *Biomass and Bioenergy*, vol. 10, no. 4, pp. 177–200, 1996, doi: 10.1016/0961-9534(95)00058-5.

[30] A. Jensen, K. Dam-Johansen, M. A. Wójtowicz, and M. A. Serio, “TG-FTIR study of the influence of potassium chloride on wheat straw pyrolysis,” *Energy and Fuels*, vol. 12, no. 5, pp. 929–938, 1998, doi: 10.1021/ef980008i.

[31] K. Raveendran, A. Ganesh, and K. C. Khilar, “Influence of mineral matter on biomass pyrolysis characteristics,” *Fuel*, vol. 74, no. 12, pp. 1812–1822, 1995, doi: 10.1016/0016-2361(95)80013.

[32] L. Han, Q. Wang, Q. Ma, C. Yu, Z. Luo, and K. Cen, “Influence of CaO additives on wheat-straw pyrolysis as determined by TG-FTIR analysis,” *J. Anal. Appl. Pyrolysis*, vol. 88, no. 2, pp. 199–206, 2010, doi: 10.1016/j.jaap.2010.04.007.

[33] W. P. Pan and G. N. Richards, “Influence of metal ions on volatile products of pyrolysis of wood,” *J. Anal. Appl. Pyrolysis*, vol. 16, no. 2, pp. 117–126, 1989, doi: 10.1016/0165-2370(89)85011-9.

[34] D. J. Nowakowski, J. M. Jones, R. M. D. Brydson, and A. B. Ross, “Potassium catalysis in the pyrolysis behaviour of short rotation willow coppice,” *Fuel*, vol. 86, no. 15, pp. 2389–2402, 2007, doi: 10.1016/j.fuel.2007.01.026.

[35] J. Billaud, S. Valin, G. Ratel, S. Thiery, and S. Salvador, “Biomass gasification between 800 and 1,400 °c in the presence of o2: Drop tube reactor experiments and simulation,” *Chem. Eng. Trans.*, vol. 37, no. 2013, pp. 163–168, 2014, doi: 10.3303/CET1437028.

[36] M. Lapuerta, J. J. Hernández, A. Pazo, and J. López, “Gasification and co-gasification of biomass wastes: Effect of the biomass origin and the gasifier operating conditions,” *Fuel Process. Technol.*, vol. 89, no. 9, pp. 828–837, 2008, doi: 10.1016/j.fuproc.2008.02.001.

[37] K. Qin, P. A. Jensen, W. Lin, and A. D. Jensen, “Biomass gasification behavior in an entrained flow reactor: Gas product distribution and soot formation,” *Energy and Fuels*, vol. 26, no. 9, pp. 5992–6002, 2012, doi: 10.1021/ef300960x.

[38] Y. Zhang, S. Kajitani, M. Ashizawa, and Y. Oki, “Tar destruction and coke formation during rapid pyrolysis and gasification of biomass in a drop-tube furnace,” *Fuel*, vol. 89, no. 2, pp. 302–309, 2010, doi: 10.1016/j.fuel.2009.08.045.

[39] J. J. Hernández, G. Aranda-Almansa, and A. Bula, “Gasification of biomass wastes in an entrained flow gasifier: Effect of the particle size and the residence time,” *Fuel Process. Technol.*, vol. 91, no. 6, pp. 681–692, 2010, doi: 10.1016/j.fuproc.2010.01.018.

[40] E. Furusjö, C. Ma, X. Ji, L. Carvalho, J. Lundgren, and E. Wetterlund, “Alkali enhanced biomass gasification with in situ S capture and novel syngas cleaning. Part 1: Gasifier performance,” *Energy*, vol. 157, no. May, pp. 96–105, 2018, doi:10.1016/j.energy.2018.05.097.

[41] M. Perander, N. DeMartini, A. Brink, J. Kramb, O. Karlström, J. Hemming, A. Moilanen, J. Konttinen, M. Hupa, “Catalytic effect of Ca and K on CO2 gasification of spruce wood char,” *Fuel*, vol. 150, pp. 464–472, 2015, doi: 10.1016/j.fuel.2015.02.062.

[42] International Organization for Standardization, “BS EN ISO 18134-3 Solid biofuels - Determination of moisture content - Oven dry method Part 3: Moisture in general analysis simple,” vol. 44, no. 0, 2014.

[43] British Standards, “BS EN 15148:2009 Solid biofuels - Method for the determination of the content of volatile matter,” *Pharmazie*, vol. 2009, pp. 1–14, 2009.

[44] International Organization for Standardization, “BS EN ISO 18122 Solid biofuels - Determination of ash content,” vol. 44, no. 0, 2014.

[45] A. A. Sluiter, R. Ruiz, C. Scarlata, J. Sluiter and D. Templeton, “Determination of Extractives in Biomass: Laboratory Analytical Procedure (LAP),” *Revue des Maladies Respiratoires*, vol. 33, no. 10. pp. 838–852, 2016, doi: 10.1016/j.rmr.2016.02.006.

[46] Rowell, R.M. (Ed.). (2012). Handbook of Wood Chemistry and Wood Composites (2nd ed.). CRC Press. https://doi.org/10.1201/b12487

[47] H. Yang, R. Yan, H. Chen, D. H. Lee, and C. Zheng, “Characteristics of hemicellulose, cellulose and lignin pyrolysis,” *Fuel*, vol. 86, no. 12–13, pp. 1781–1788, Aug. 2007, doi: 10.1016/j.fuel.2006.12.013.

[48] T. Mani, P. Murugan, J. Abedi, and N. Mahinpey, “Pyrolysis of wheat straw in a thermogravimetric analyzer: Effect of particle size and heating rate on devolatilization and estimation of global kinetics,” *Chem. Eng. Res. Des.*, vol. 88, no. 8A, pp. 952–958, 2010, [Online]. Available: https://www.cheric.org/research/tech/periodicals/view.php?seq=852663.

[49] E. Biagini, F. Barontini, and L. Tognotti, “Devolatilization of Biomass Fuels and Biomass Components Studied by TG/FTIR Technique,” *Ind. Eng. Chem. Res.*, vol. 45, no. 13, pp. 4486–4493, Jun. 2006, doi: 10.1021/ie0514049.